

Applications of Image Translation Methods Based on Deep Learning to Solar Data

Eunsu Park

Kyung Hee University, South Korea / espark@khu.ac.kr

0

Introduction

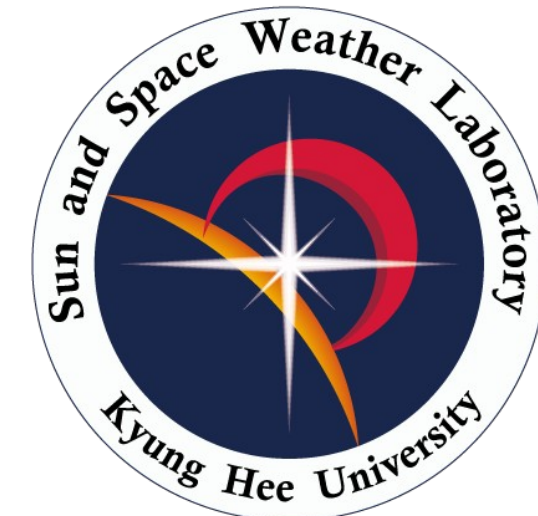
Sun and Space Weather Group in Kyung Hee University

We have applied deep learning (DL) to various types of solar and space weather data and tasks

Our goal:

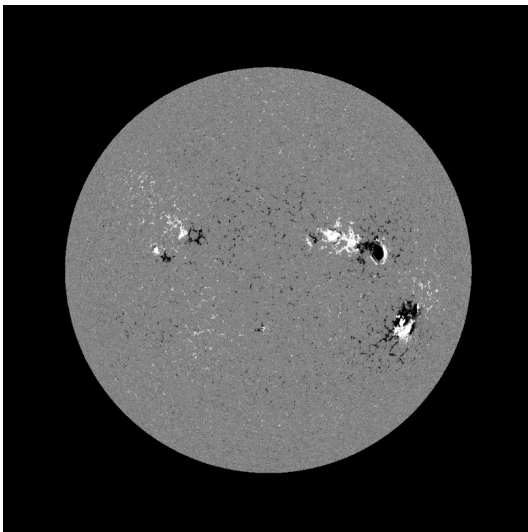
- 1) To improve space weather prediction models
- 2) To fill in observation blanks
- 3) To calibrate observational data such as denoising
- 4) To study whether DL-generated data are feasible for scientific data or not

Recently, we have applied image translation methods based on deep learning to various solar and space weather data.

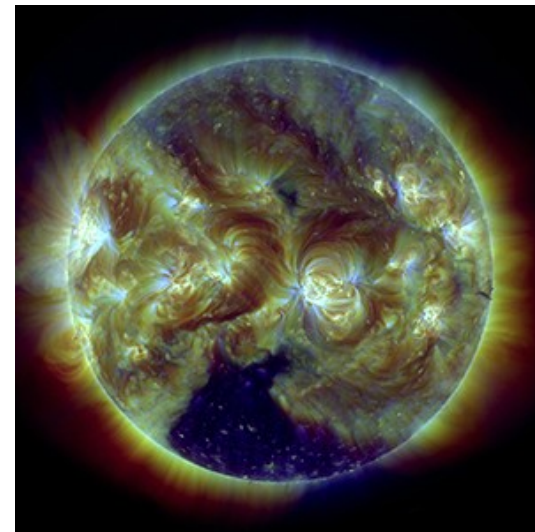


Why image translation?

Magnetogram



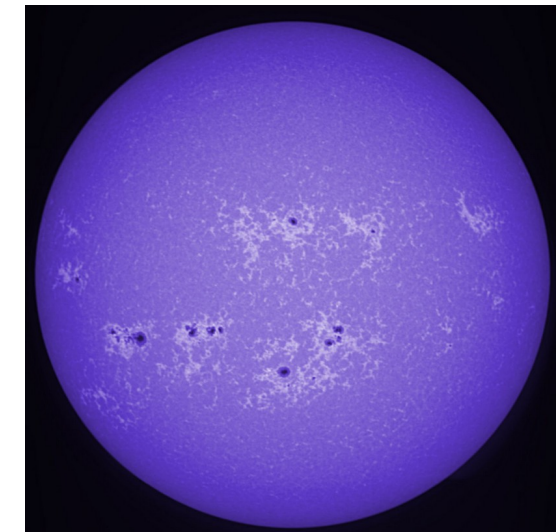
EUV



H-alpha



Ca K



There are various types of multi-filter observations in solar and space weather, and many of them are observed simultaneously.

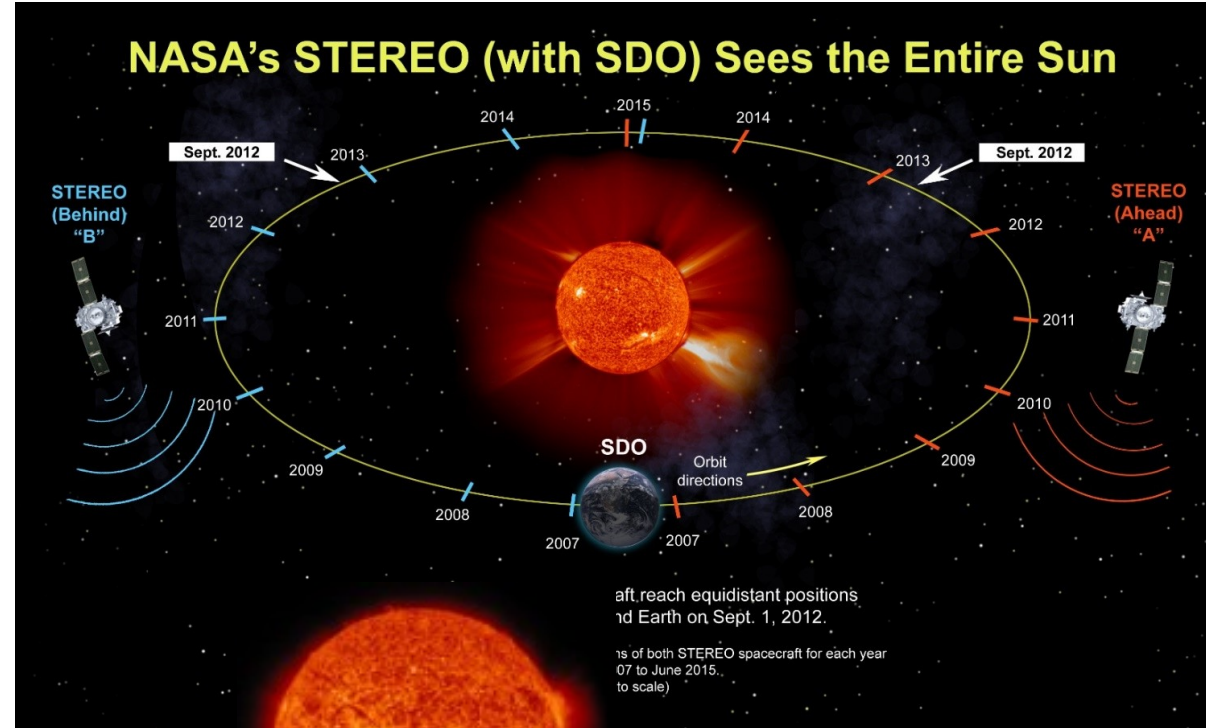
-> It is a good condition for applying the image translation algorithms.

1

Generation of Solar Far-side Magnetograms from STEREO/EUVI Images

**Kim, Park, Lee et al., 2019
Jeong et al., 2020
Park et al., 2021**

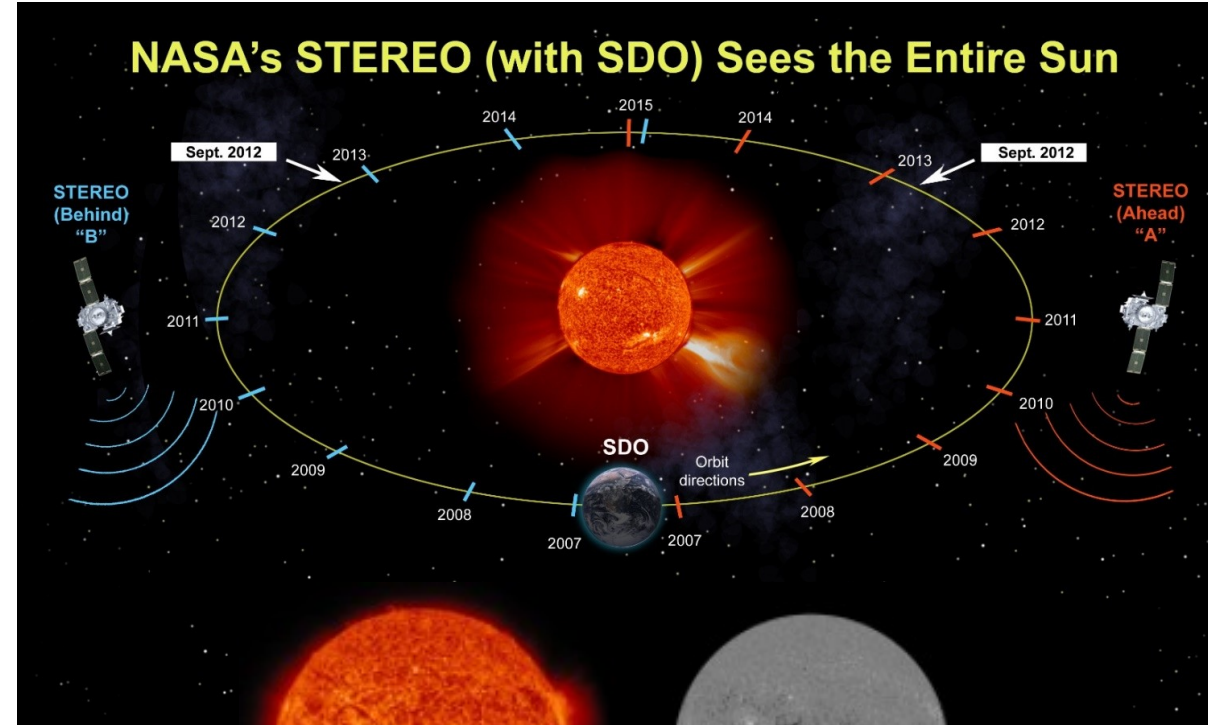
Generation of Solar Farside Magnetograms



Solar EUV images are being observed from the front and farside of the Sun



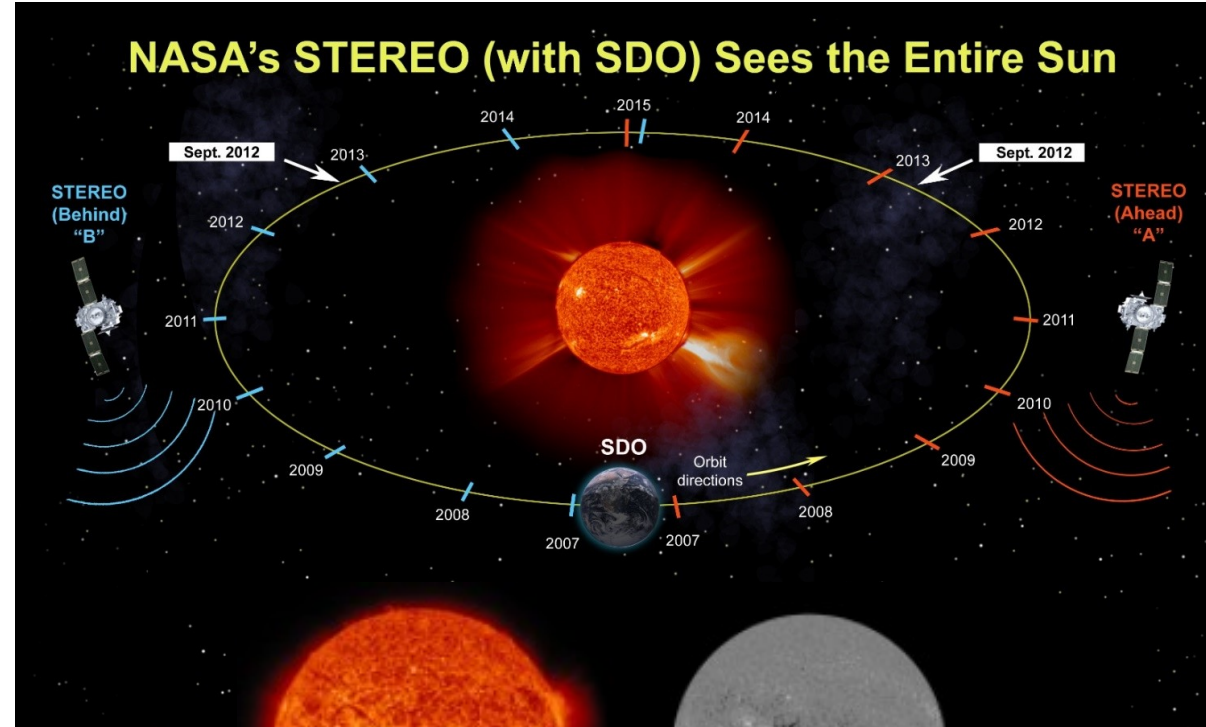
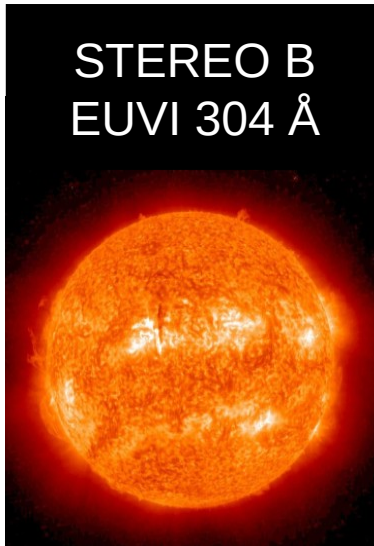
Generation of Solar Farside Magnetograms



Solar EUV images are being observed from the front and farside of the Sun

Solar magnetograms are limited to the frontside solar disk

Generation of Solar Farside Magnetograms



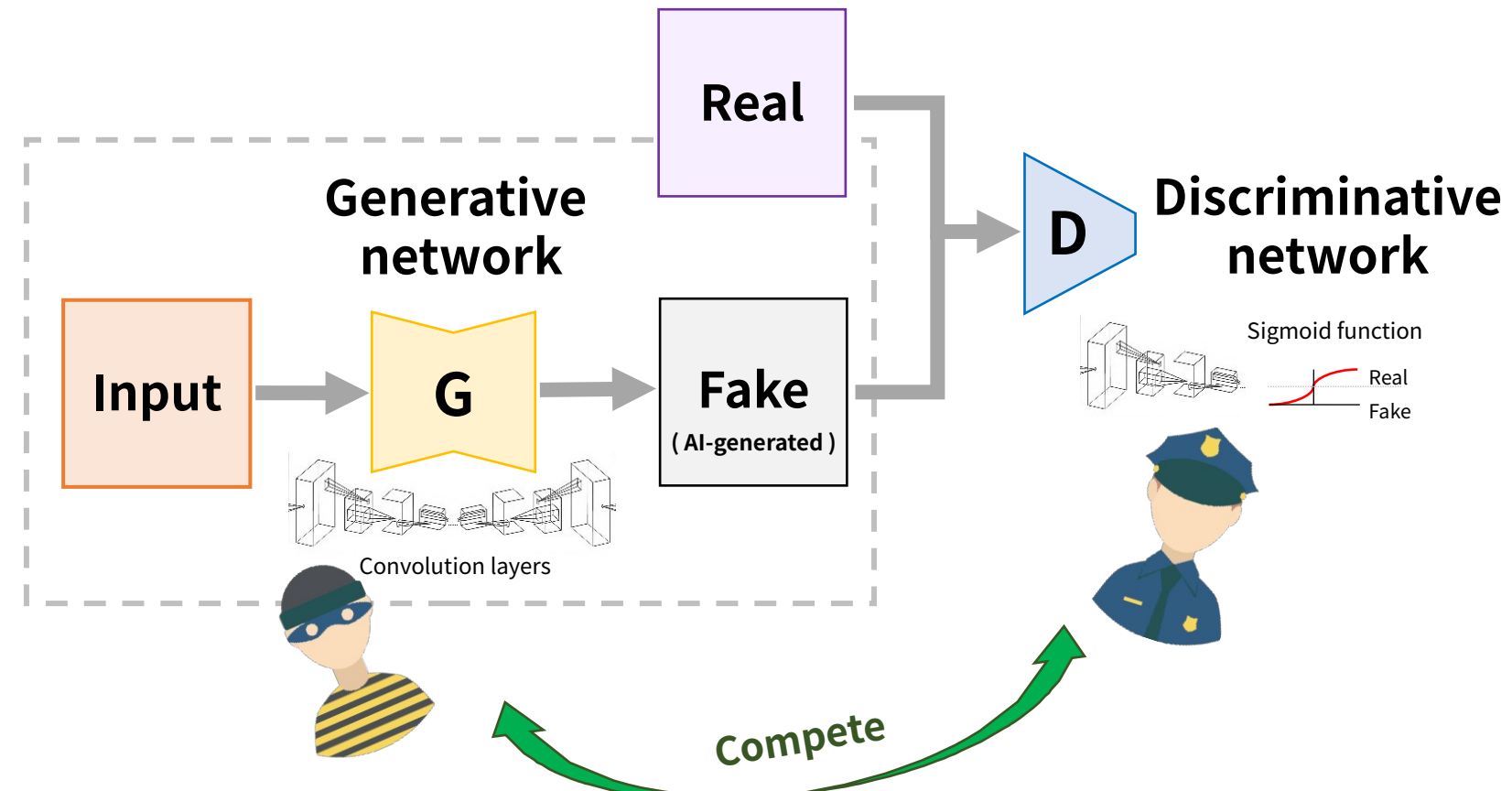
Solar EUV images are being observed from the front and farside of the Sun

Solar magnetograms are limited to the frontside solar disk

We design a model for the translation from solar EUV images to solar magnetograms

Generation of Solar Farside Magnetograms

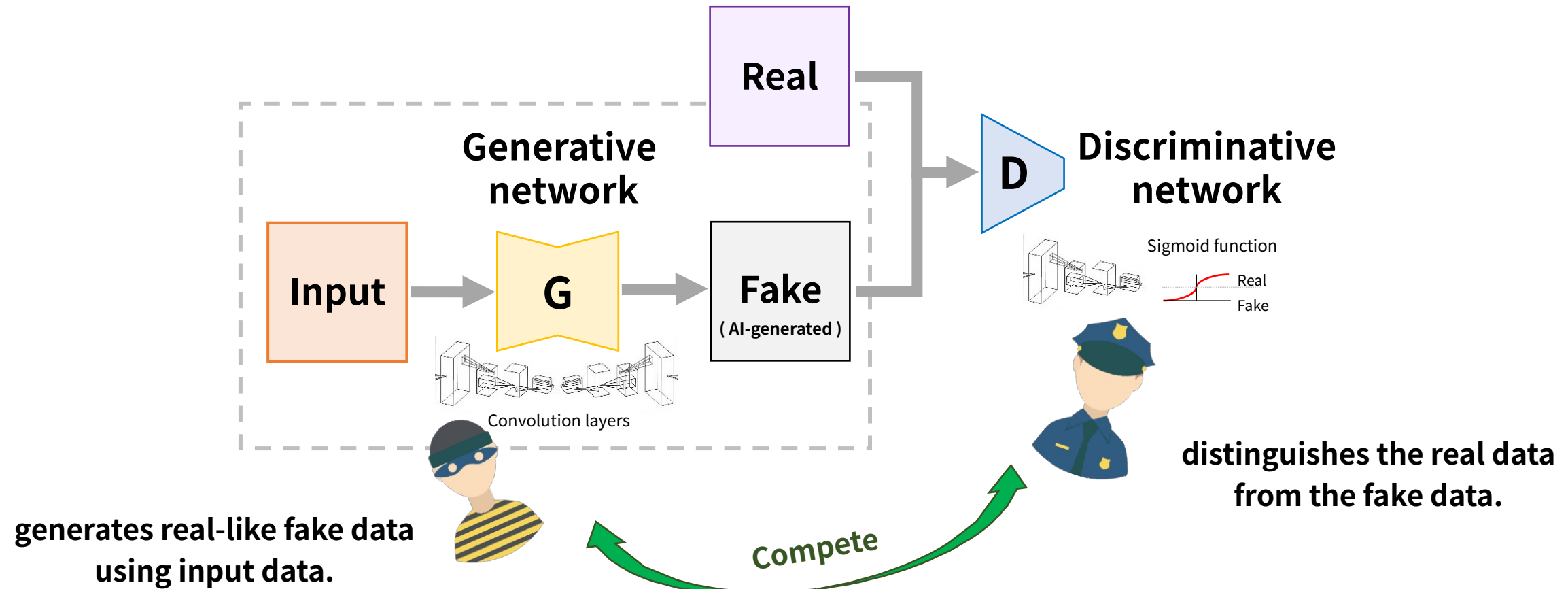
Generative Adversarial Network (GAN)



GAN is one of the popular deep learning methods in generation and translation tasks.

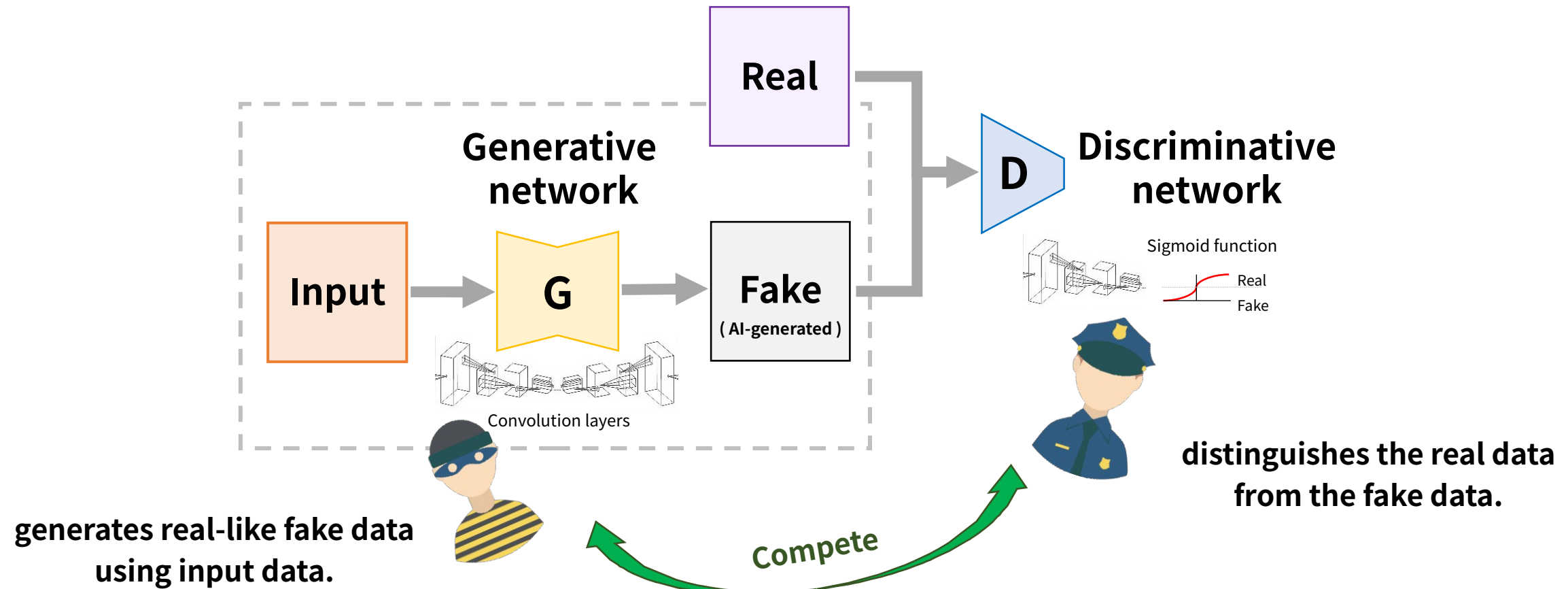
Generation of Solar Farside Magnetograms

Generative Adversarial Network (GAN)



Generation of Solar Farside Magnetograms

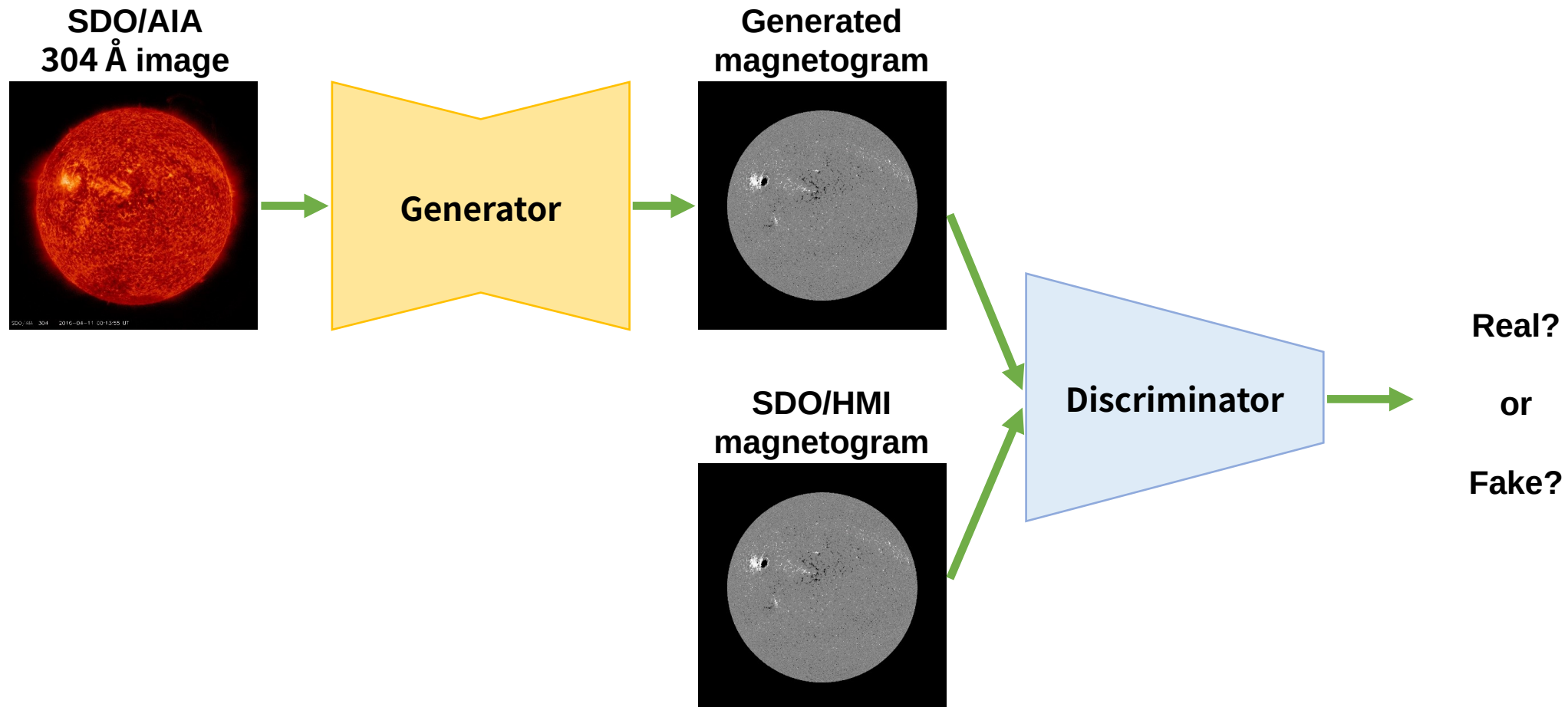
Generative Adversarial Network (GAN)



We train the Generator and the Discriminator, this process looks like a competition between the two networks.

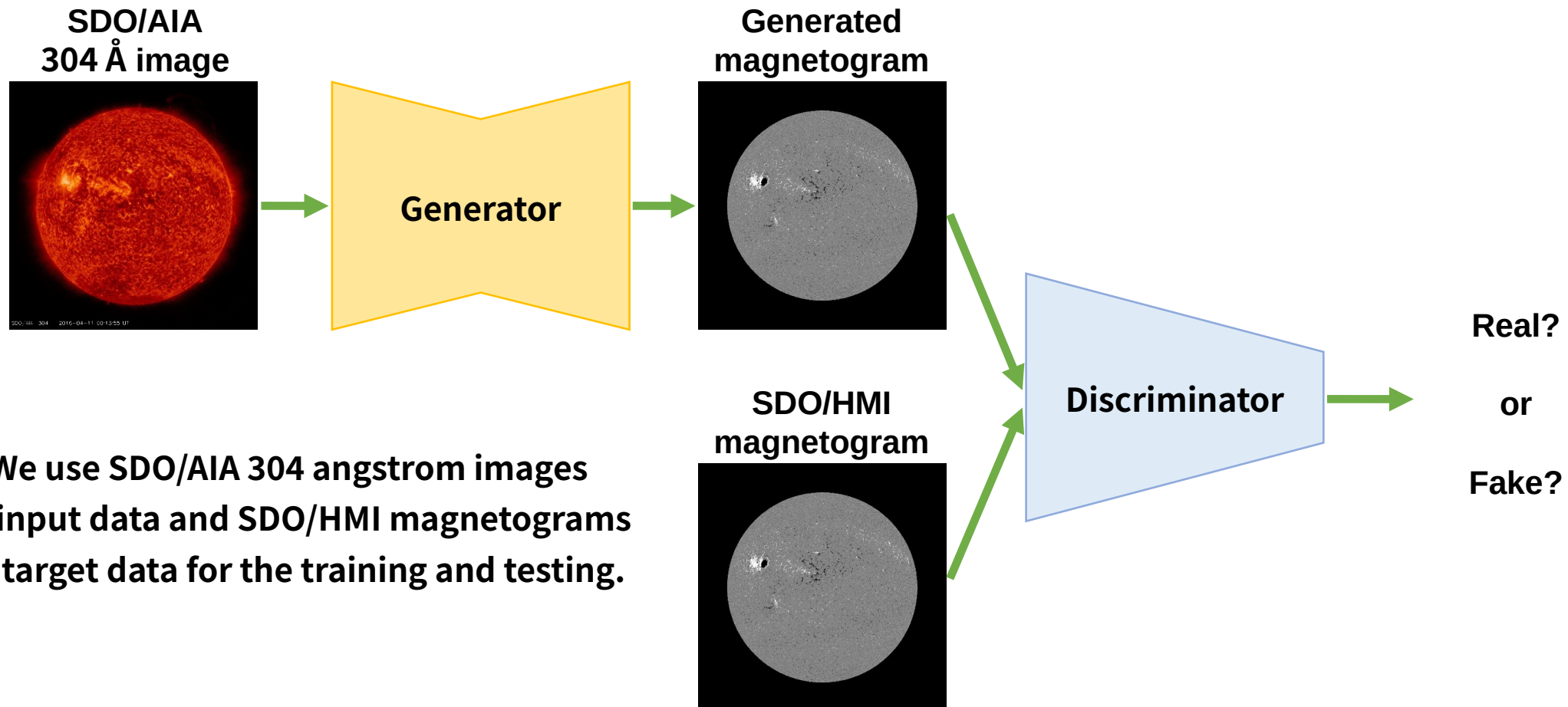
Generation of Solar Farside Magnetograms

Structure of our model for the translation from solar EUV images to solar magnetograms



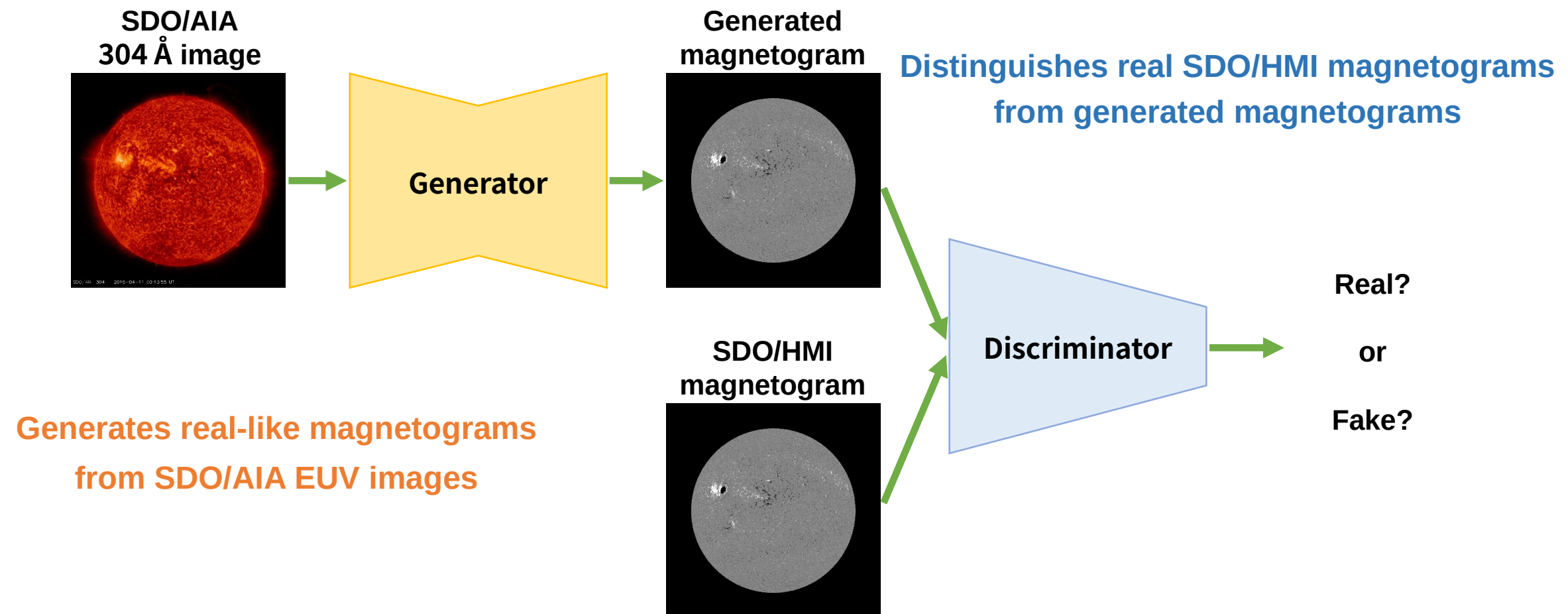
Generation of Solar Farside Magnetograms

Structure of our model for the translation from solar EUV images to solar magnetograms



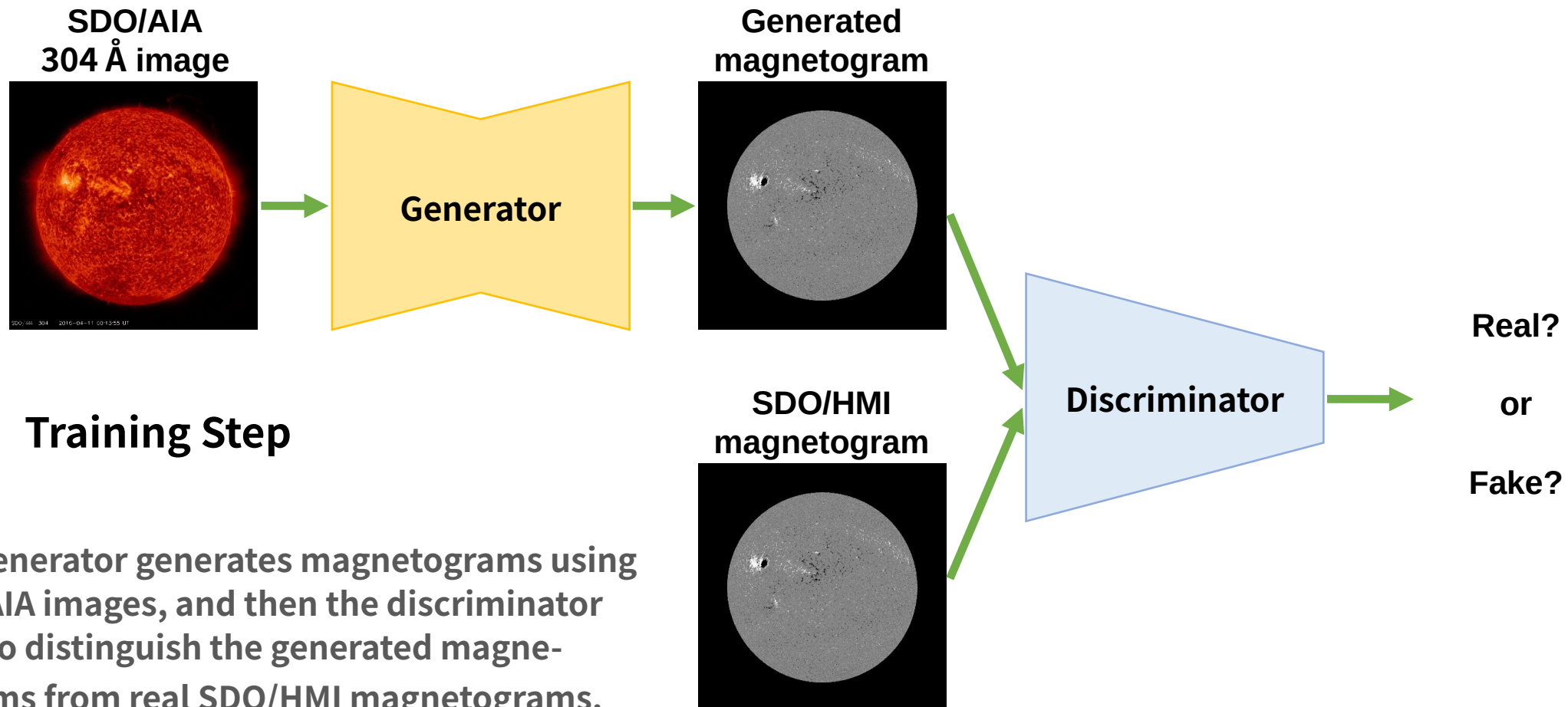
Generation of Solar Farside Magnetograms

Structure of our model for the translation from solar EUV images to solar magnetograms



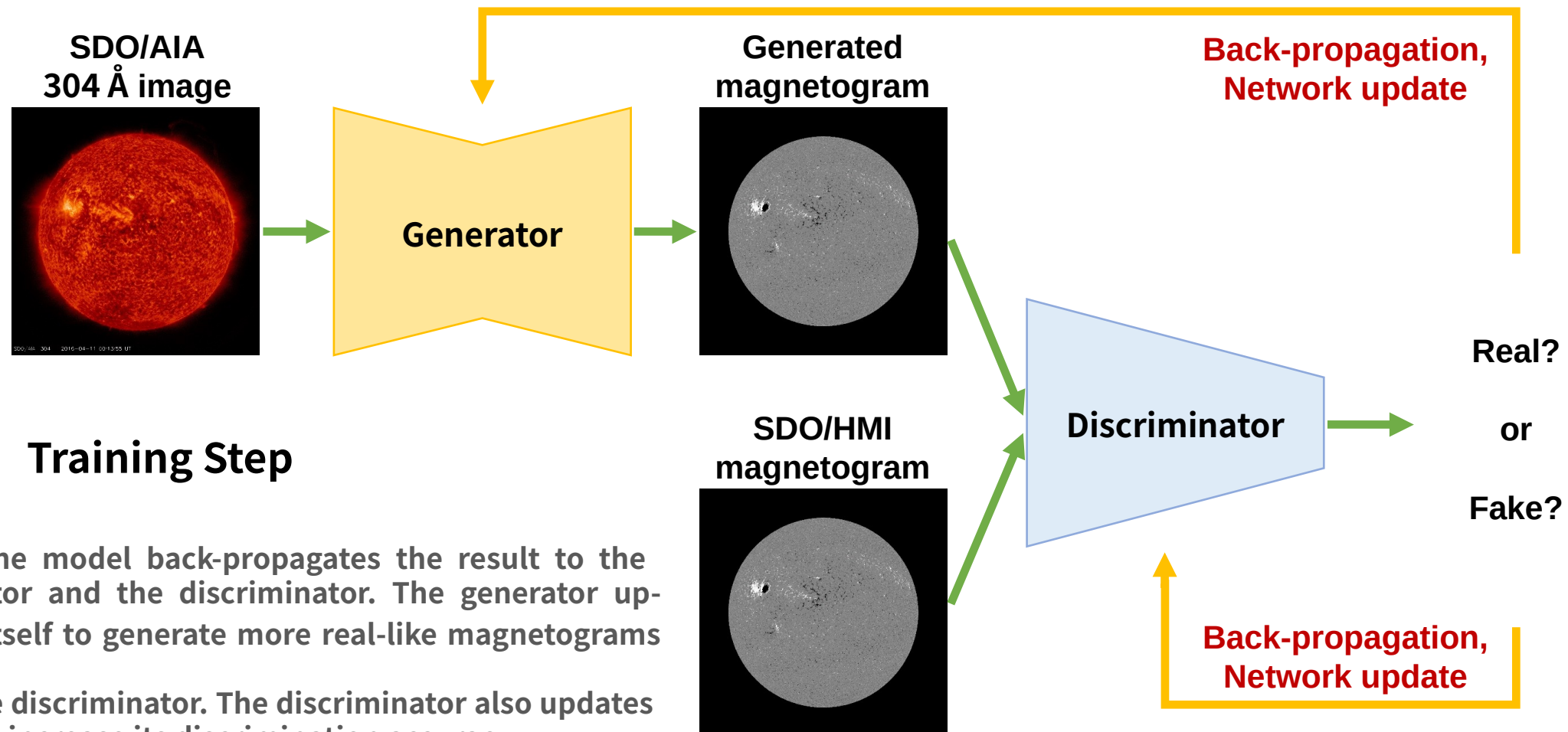
Generation of Solar Farside Magnetograms

Structure of our model for the translation from solar EUV images to solar magnetograms



Generation of Solar Farside Magnetograms

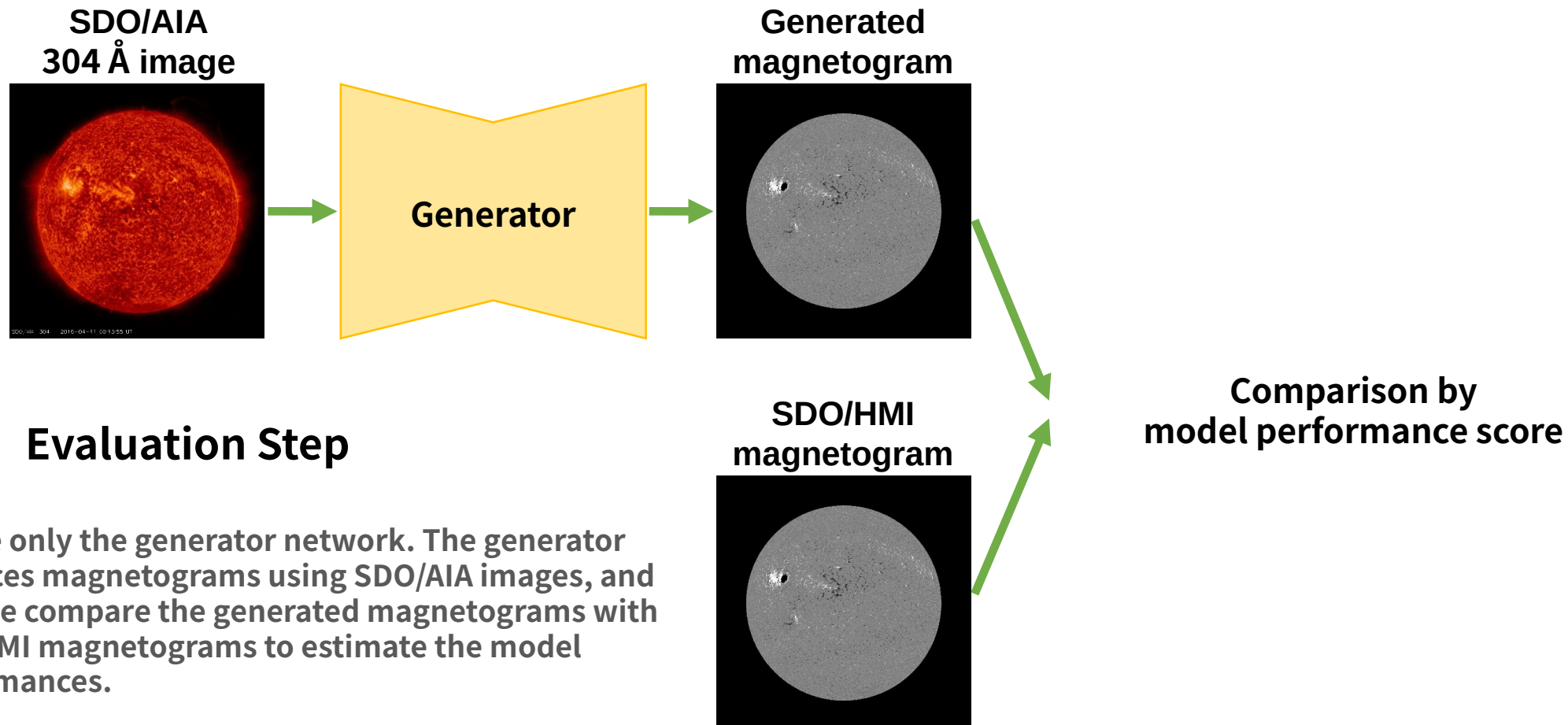
Structure of our model for the translation from solar EUV images to solar magnetograms



Then the model back-propagates the result to the generator and the discriminator. The generator updates itself to generate more real-like magnetograms to fool the discriminator. The discriminator also updates itself to increase its discrimination accuracy.

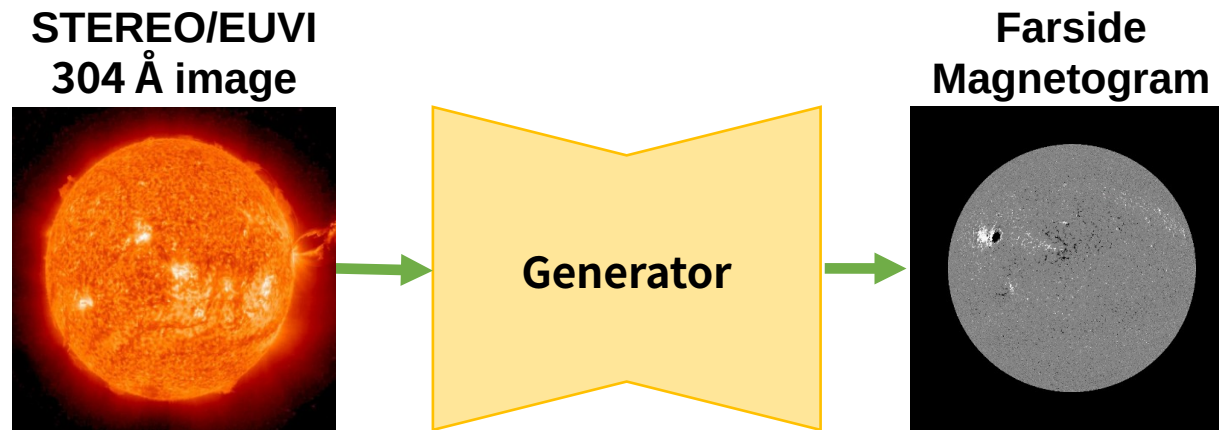
Generation of Solar Farside Magnetograms

Structure of our model for the translation from solar EUV images to solar magnetograms



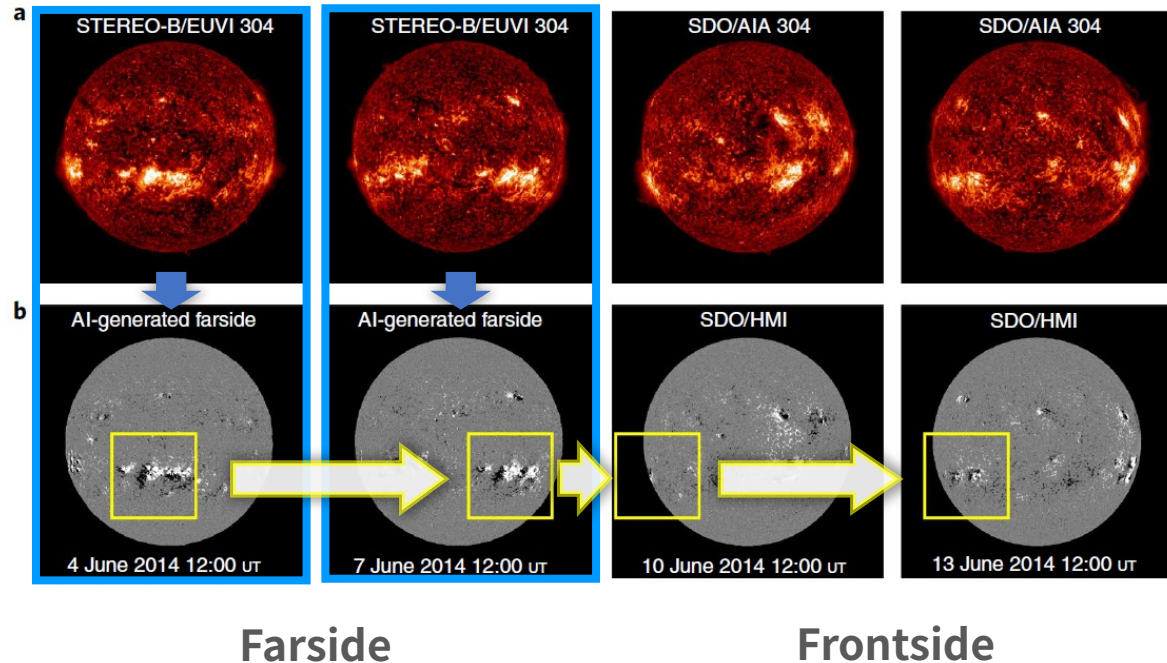
Generation of Solar Farside Magnetograms

Structure of our model for the translation from solar EUV images to solar magnetograms



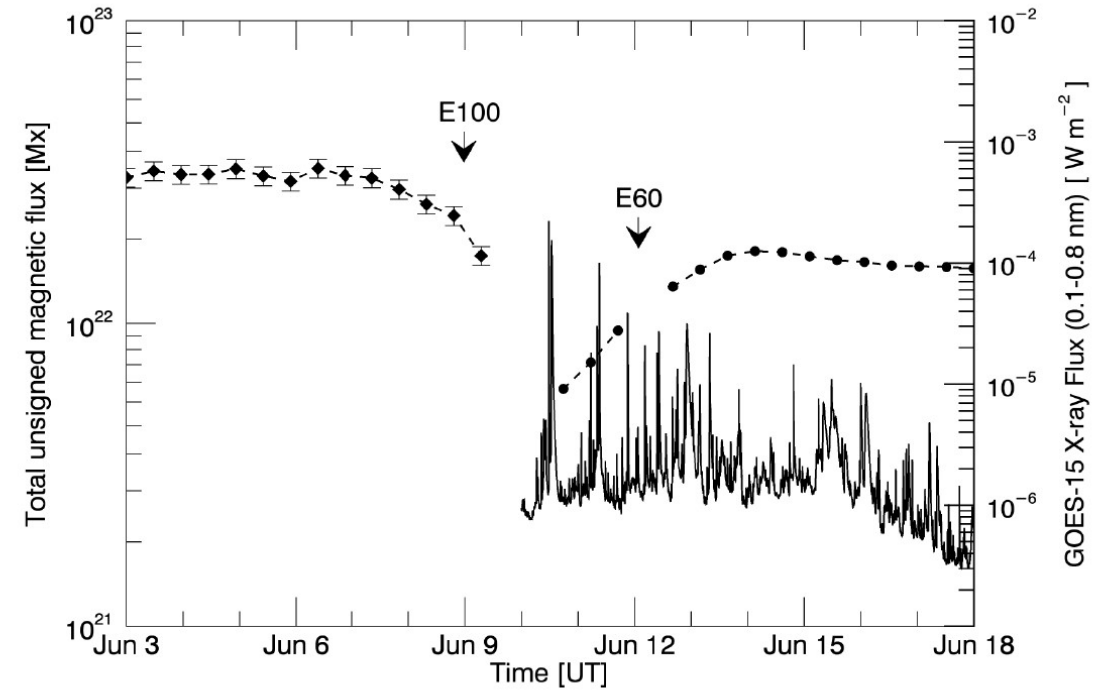
Generation Step

Generation of Solar Farside Magnetograms



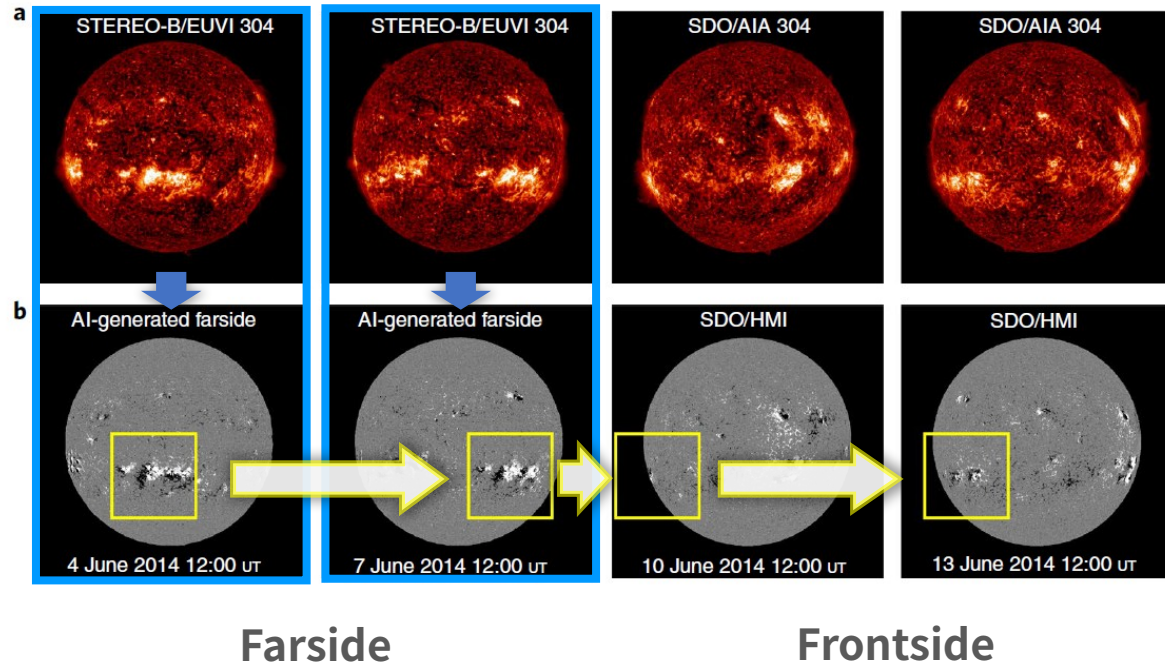
Time Series Images from farside to frontside

Kim, Park, Lee et al. (2019) suggest a deep learning model for generating solar farside magnetograms from STEREO/EUVI observations. The result shows that we could monitor the temporal evolution of magnetic fields from the solar far side to the solar front side using DL-generated data.



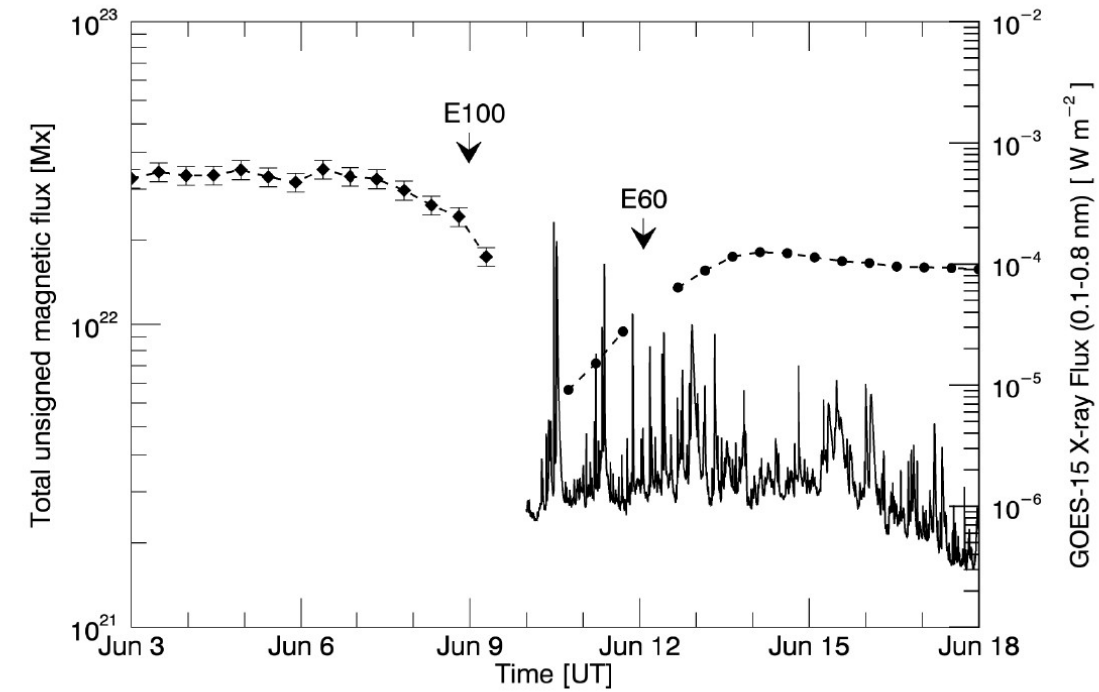
A temporal evolution of total unsigned magnetic flux of the NOAA AR 12087 from June 3 to 19 2014

Generation of Solar Farside Magnetograms



Time Series Images from farside to frontside

However, this study is limited to the maximum magnetic field strength of 100 G and shows low correlations in solar quiet regions.

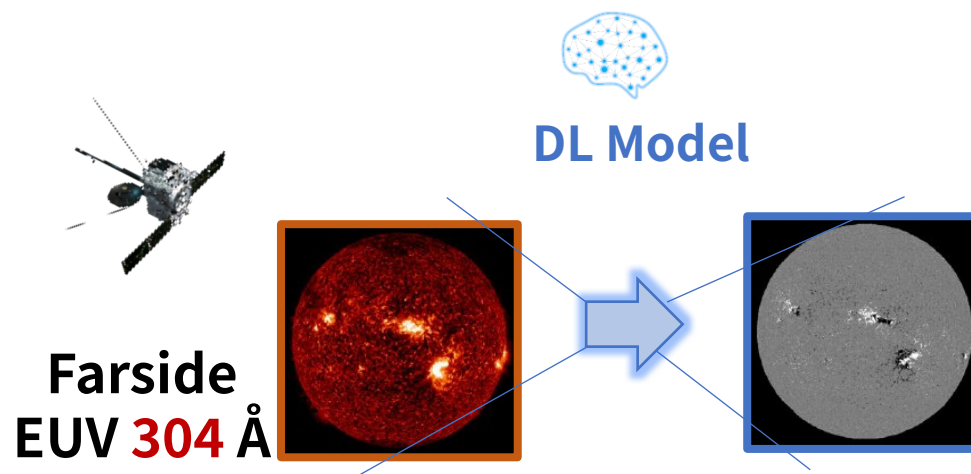


A temporal evolution of total unsigned magnetic flux of the NOAA AR 12087 from June 3 to 19 2014

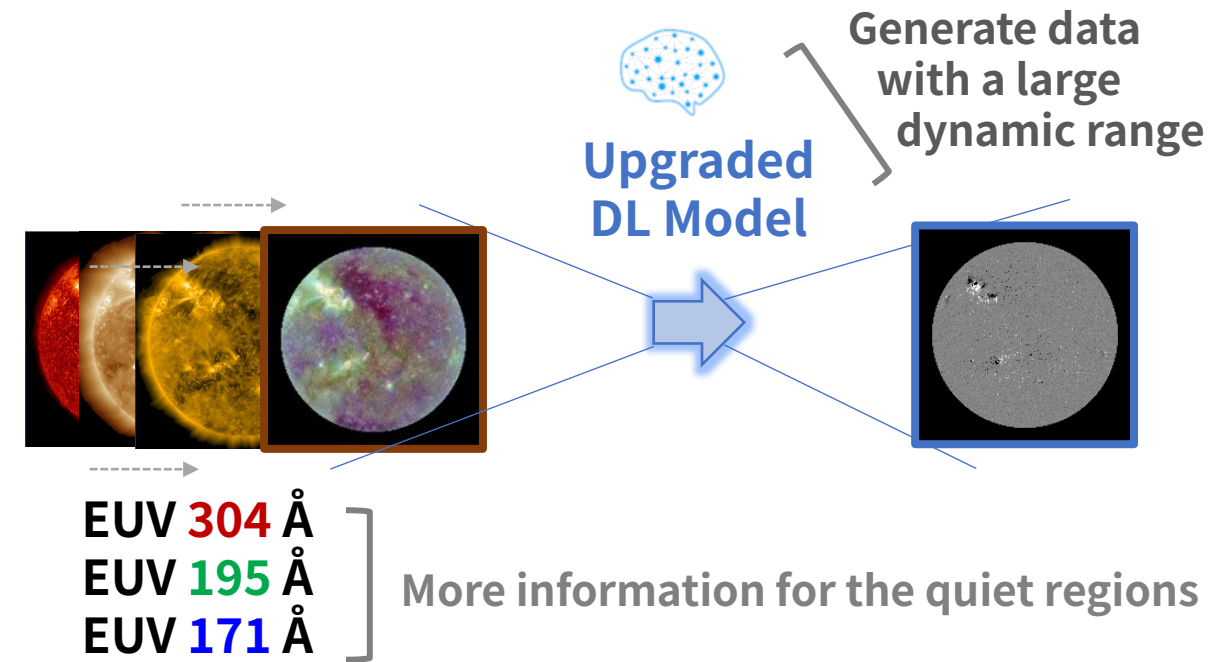
Generation of Solar Farside Magnetograms

AISFM* Ver 1.0

* AI-generated Solar Farside Magnetogram



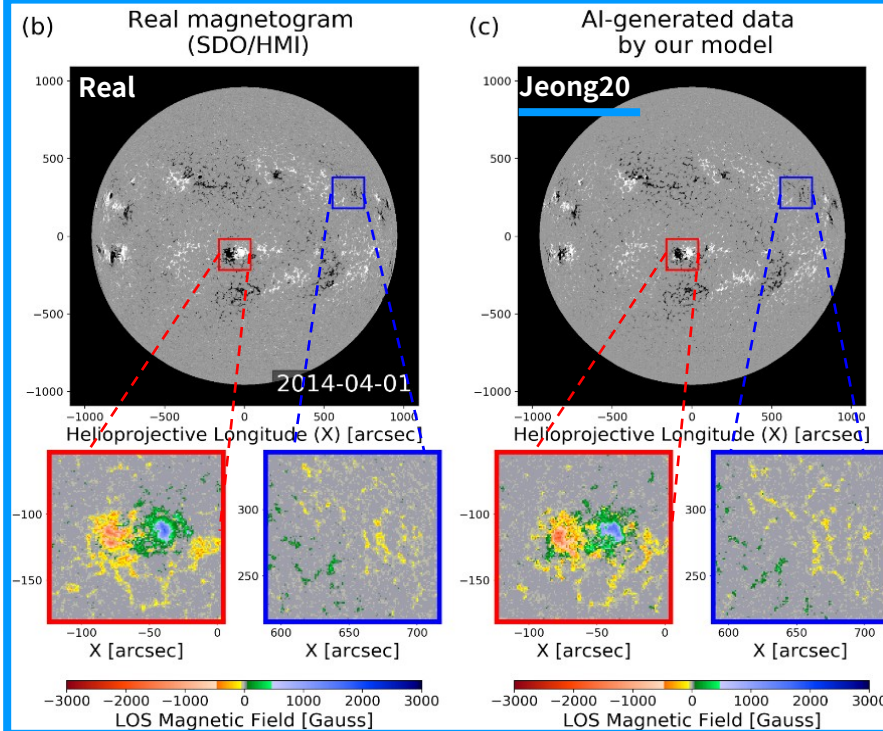
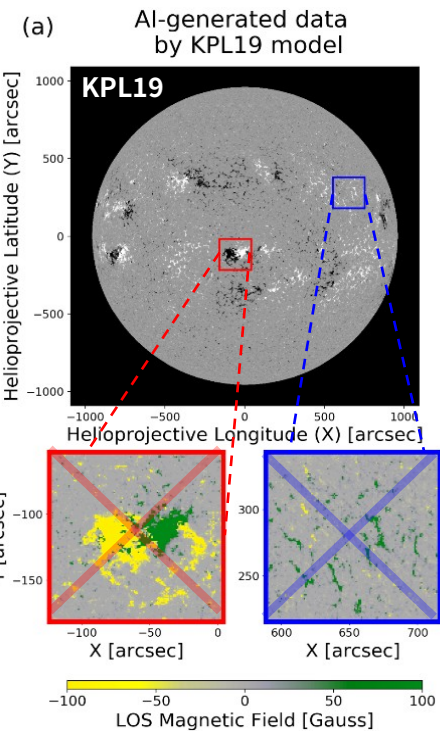
AISFM Ver 2.0



Jeong et al. (2020) upgrade the model with 3,000 Gauss dynamic range to generate more realistic magnetic fluxes, and with multi-channel input to improve the generation of quiet regions.

Generation of Solar Farside Magnetograms

AISFM* Ver 1.0



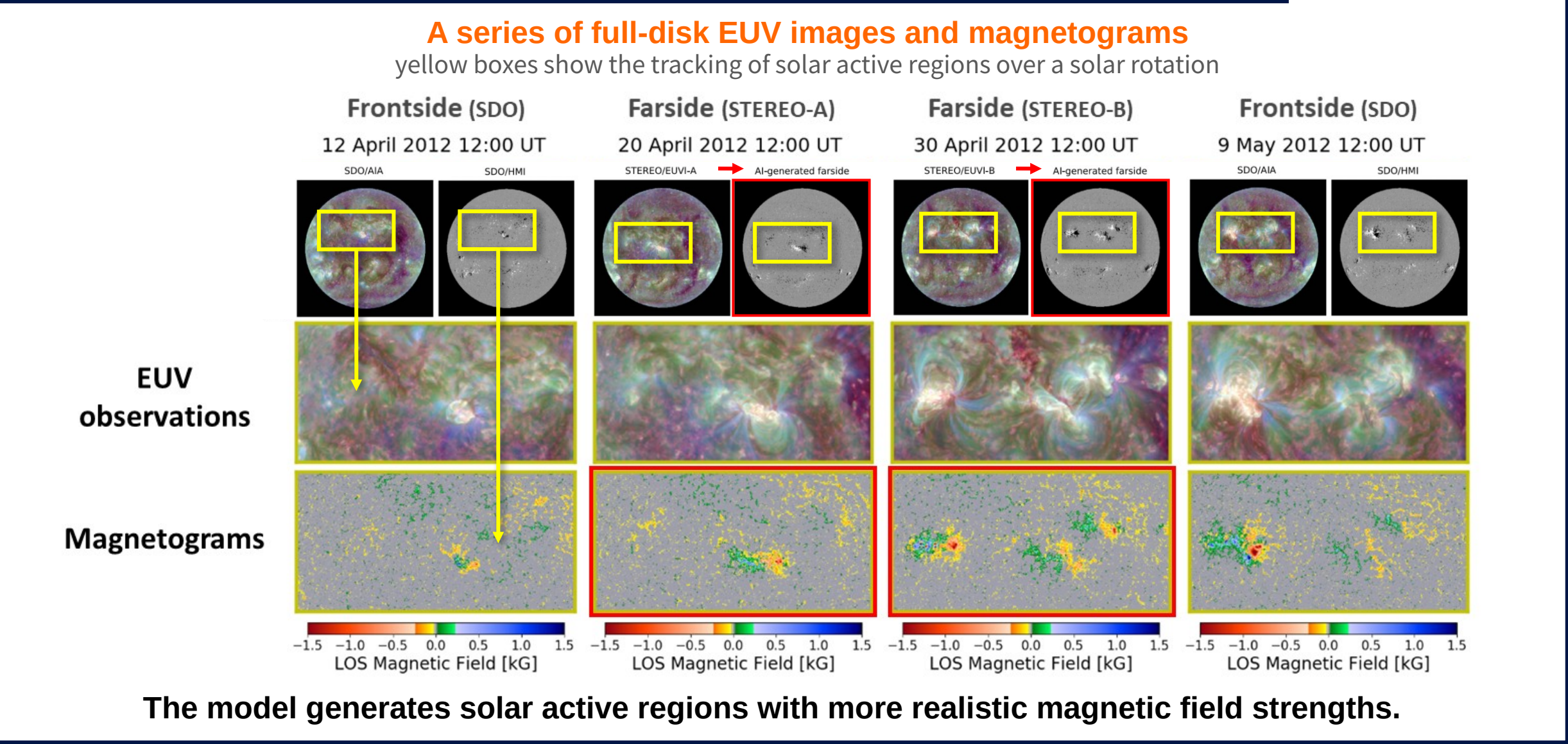
AISFM Ver 2.0

Three Objective Measures of Comparison between SDO/HMI Magnetograms and AI-generated Ones for Full Disk, ARs, and QRs

	Full Disk		AR		QR	
	825 images (1,024 × 1,024 pixels)		1,033 patches (128 × 128 pixels)		825 patches (128 × 128 pixels)	
	Ours	KPL19	Ours	KPL19	Ours	KPL19
Total unsigned magnetic flux CC	0.99	0.97	0.95	0.95	0.98	0.74
Net magnetic flux CC	0.86	...	0.93	...	0.97	...
Mean pixel-to-pixel CC (8 × 8 binning)	0.81	0.77	0.79	0.66	0.62	0.21

The model (AISFM Ver 2.0) generates both the active and quiet regions more realistically than the previous model (AISFM Ver 1.0) and shows better results in quantitative comparisons.

Generation of Solar Farside Magnetograms

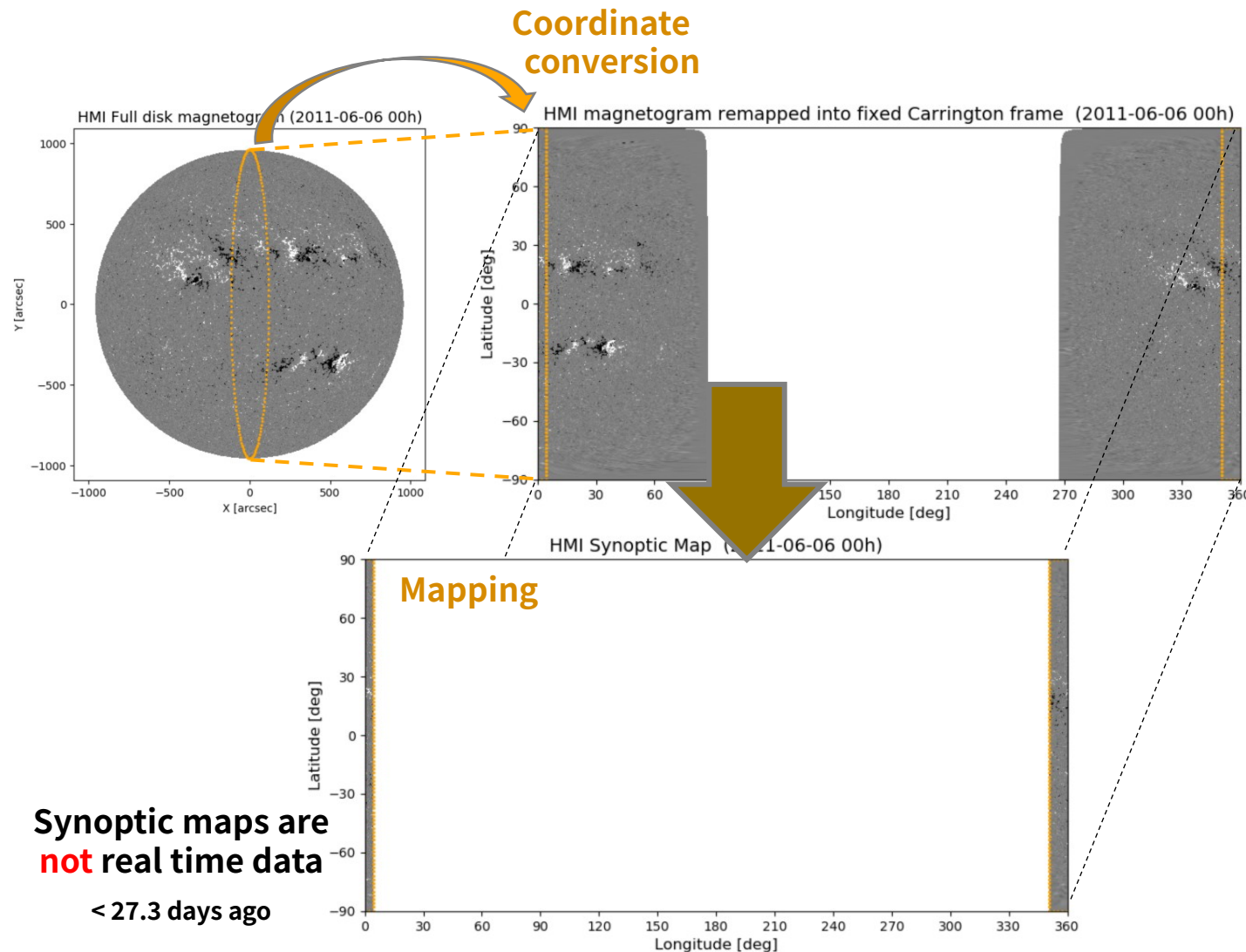


Generation of Solar Farside Magnetograms

Conventional Synoptic Map

Conventional magnetic field synoptic maps have been constructed by merging frontside magnetograms over a 27 day solar rotation period because there is no magnetogram in solar farside.

The conventional synoptic maps are **not based on real-time** ones.

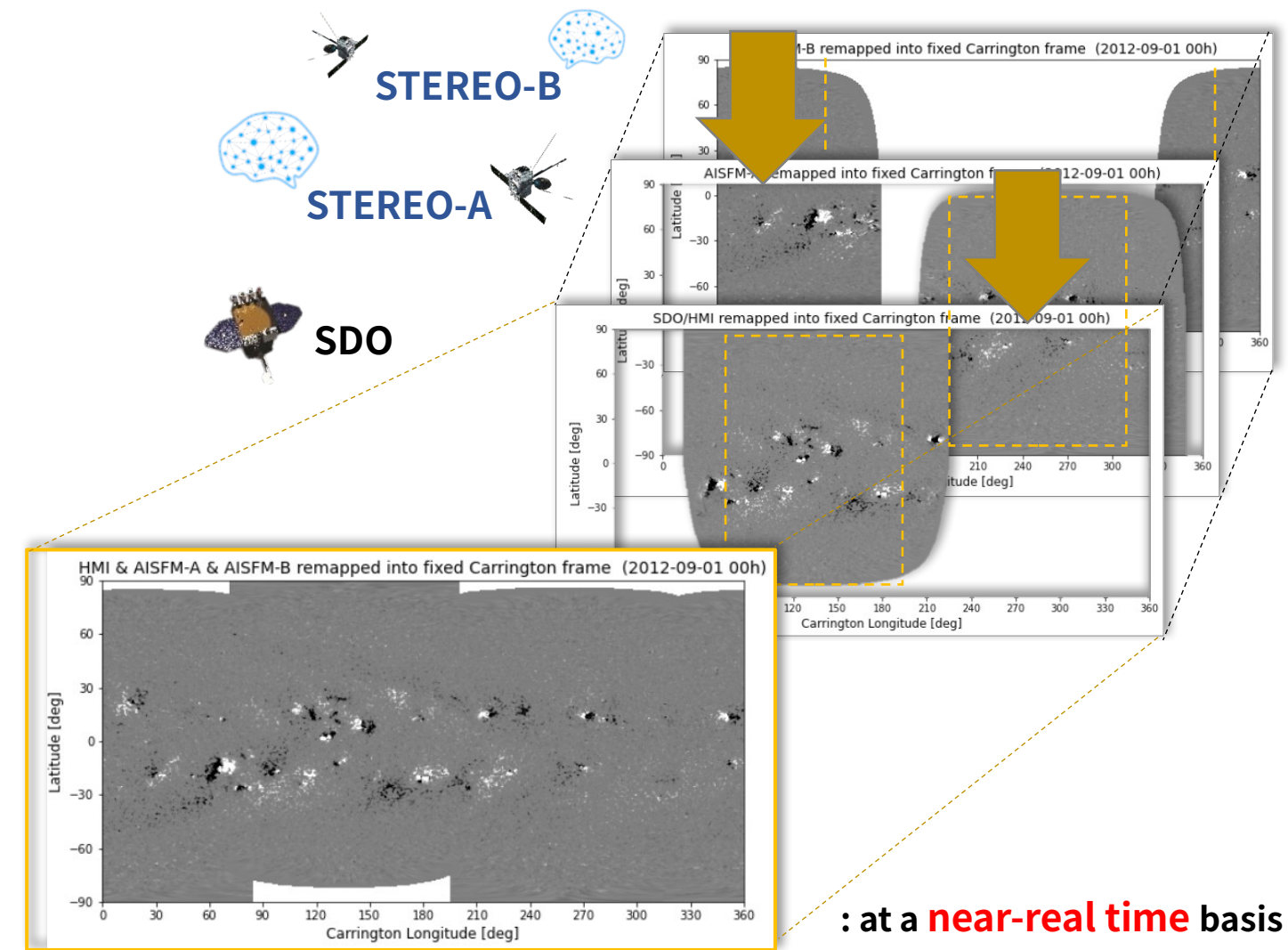


Generation of Solar Farside Magnetograms

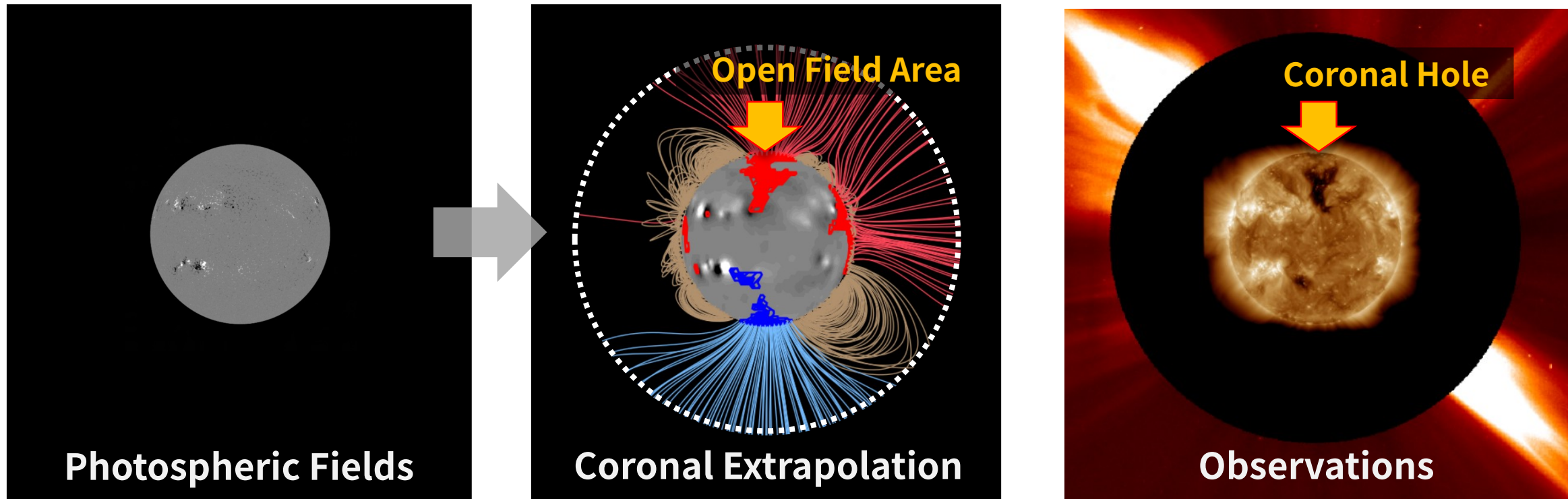
HMI & AI Synchronic Map

We construct AI synchronic global magnetic field maps by merging the farside magnetograms and SDO/HMI magnetograms.

These AI synchronic maps can cover mostly real-time global solar photospheric fields.



Generation of Solar Farside Magnetograms

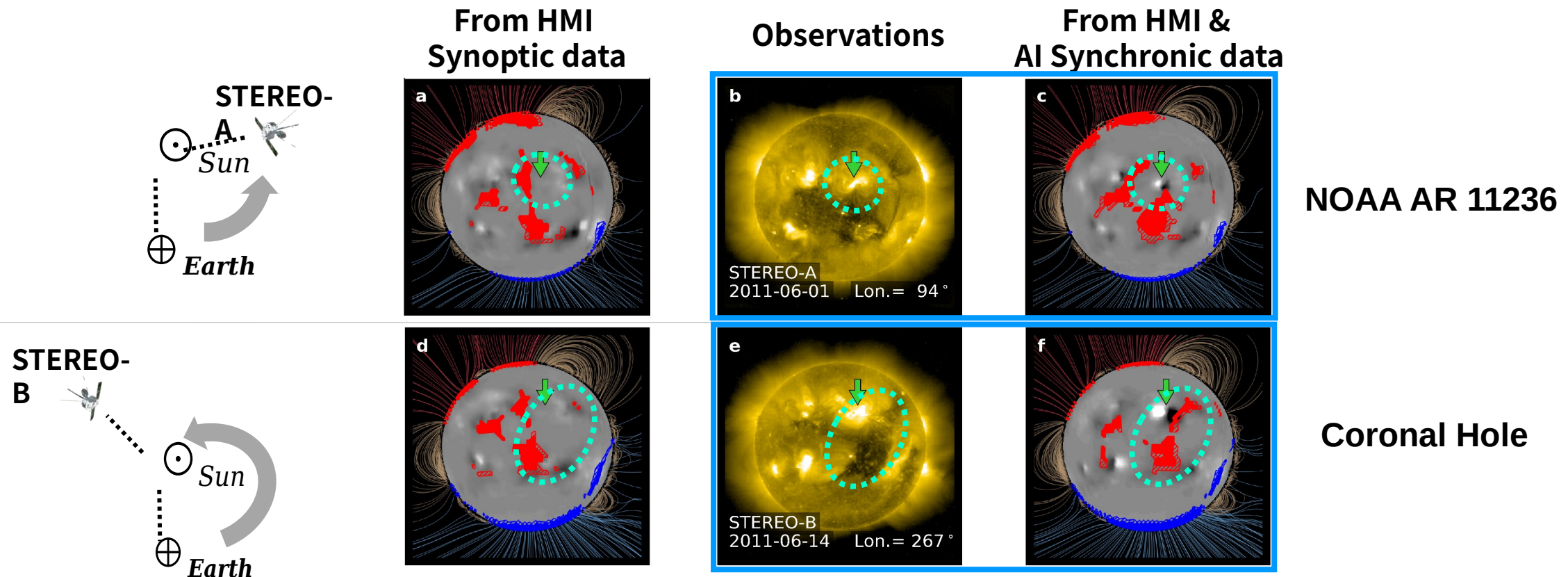


We extrapolate the global coronal magnetic field from the AI synchronic maps using **Potential Field Source Surface (PFSS)** model, then compare the results with coronal observations.

Open field lines, which are computed by the PFSS model, arriving at the source surface are associated with coronal holes.

Generation of Solar Farside Magnetograms

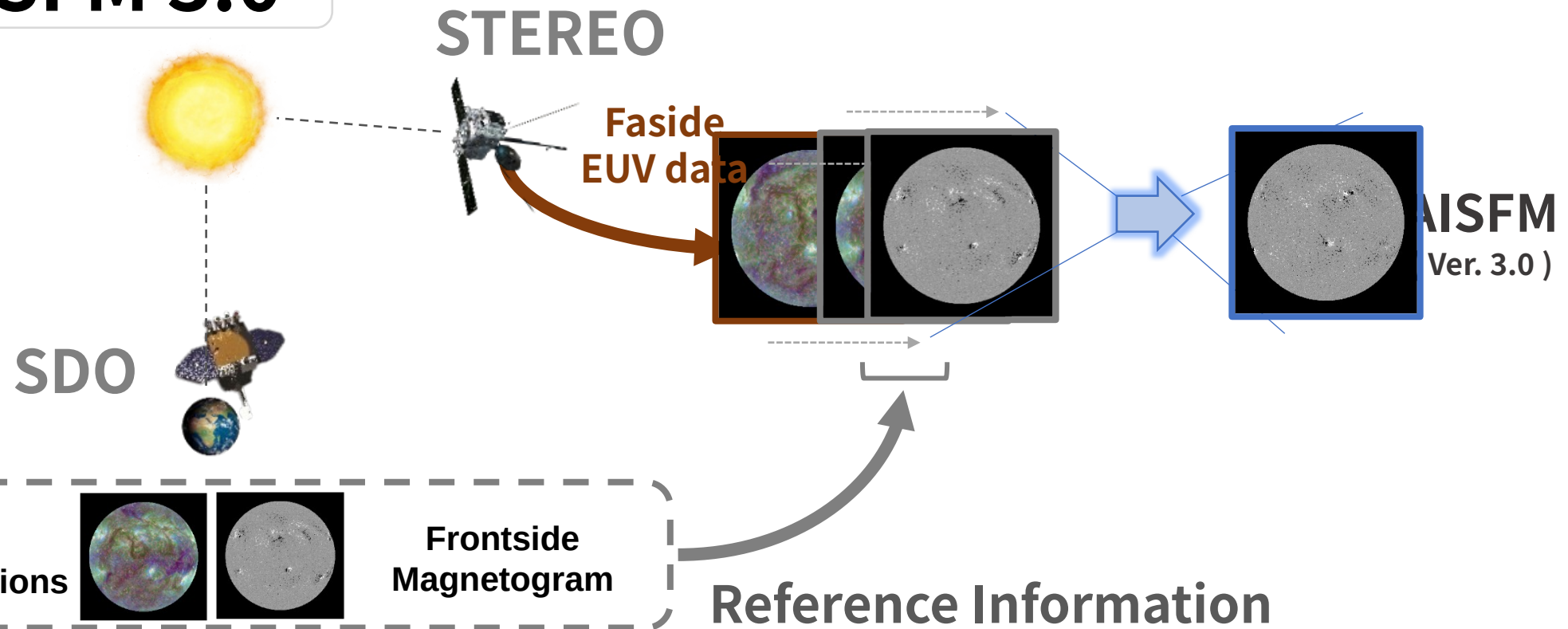
Comparison between farside solar EUV observations and results of PFSS extrapolations



The extrapolation results using AI synchronic data well represent the appearance of the active region and the coronal hole, and the results agree with the observations.

Generation of Solar Farside Magnetograms

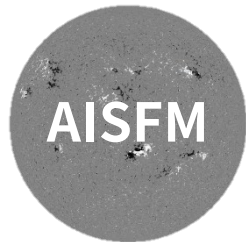
AISFM 3.0



We are trying to improve our model by providing **solar frontside data** to the model as **reference information**.

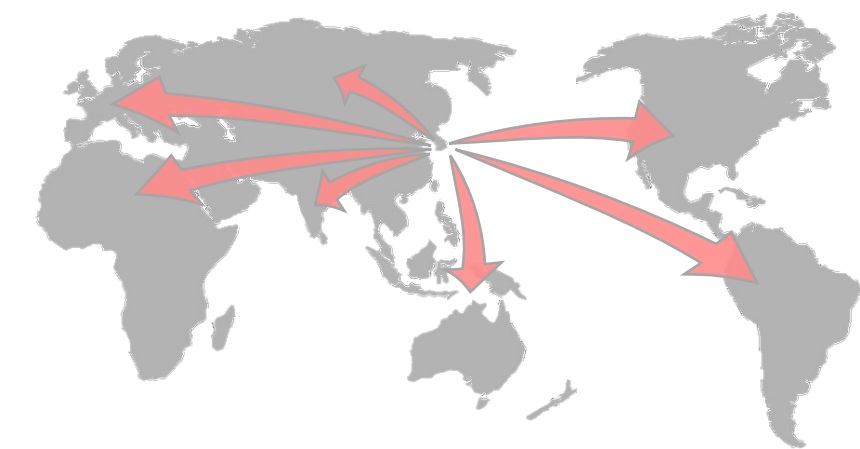
Generation of Solar Farside Magnetograms

Public release of solar farside magnetograms soon



- A: 2011.01 ~ 2019.12 (~ 47 GB)
- B: 2011.01 ~ 2014.09 (~ 21 GB)

2011.01 ~ 2019.12 (~ 26 GB)



We are going to release the solar farside magnetograms and AI synchronic maps through Korean Data Center (KDC) for SDO in Korean Astronomy and Space Science Institute (KASI).



KDC for SDO in KASI

2

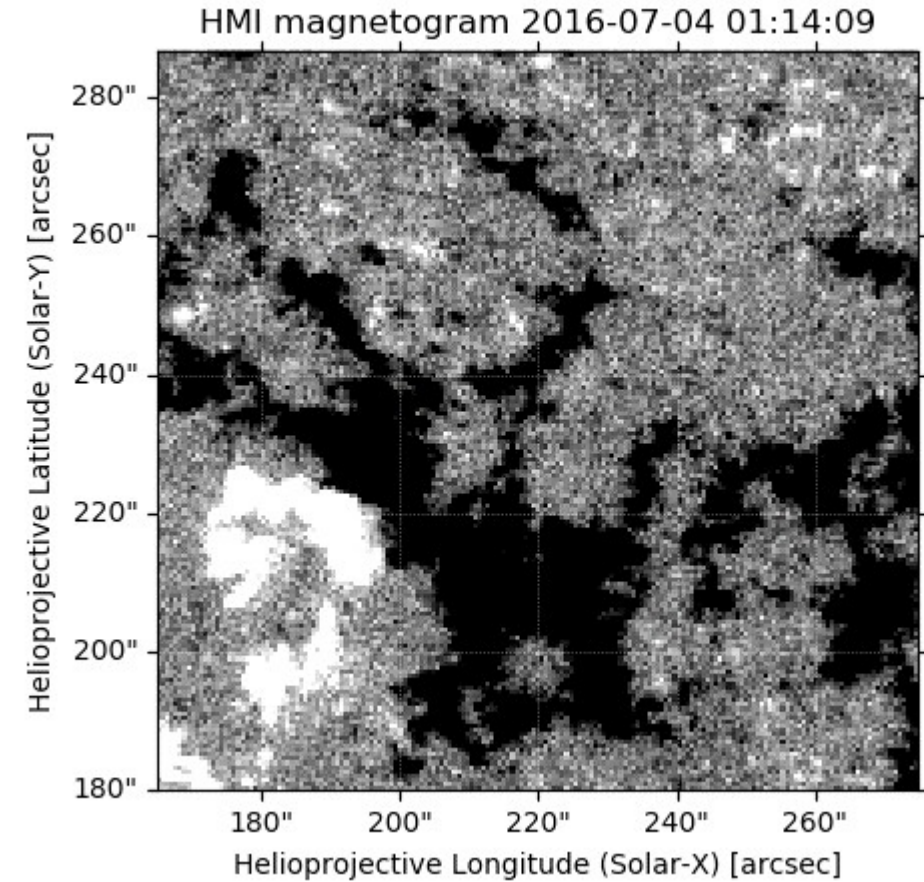
De-noising SDO/HMI Magnetograms

Park et al., 2020

Denoising SDO/HMI Magnetogram

Liu+ (2012) reported that

“An upper bound to the random noise for the 1” resolution **HMI 45-second magnetograms is 10.2 G**, and **6.3 G for the 720-second magnetograms.**”

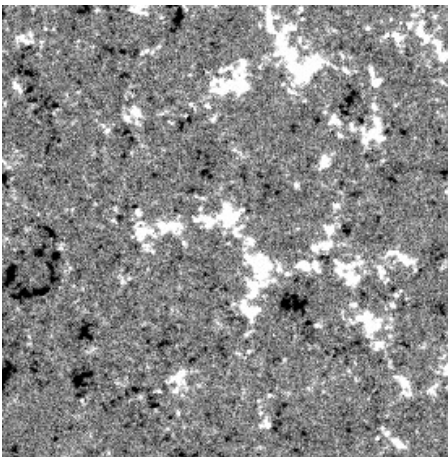


Denoising SDO/HMI Magnetogram

- Several studies investigated weak solar magnetic field structures such as solar intra-network and small bi-poles by integrating magnetic field observations to increase the signal-to-noise ratio (Wang et al. 1995; Schrijver et al. 1997; Chae et al. 2001).
- Several studies tried to reduce the noise level of solar magnetograms by several types of computing algorithms (DeForest 2017; DiasBaso et al. 2019).
- In this study, we apply two deep learning methods to denoising SDO/HMI magnetograms.

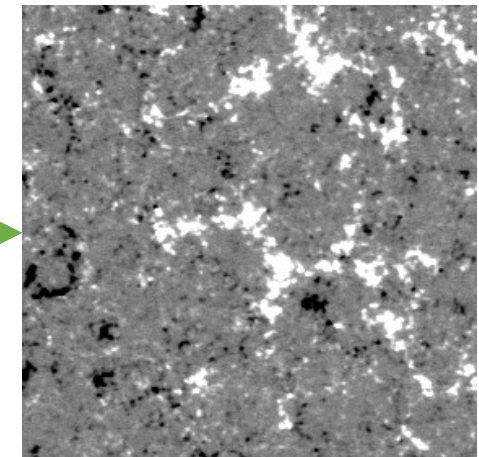
Denoising SDO/HMI Magnetogram

Original HMI
(Input)



DL Model

Denoised HMI
(Target)



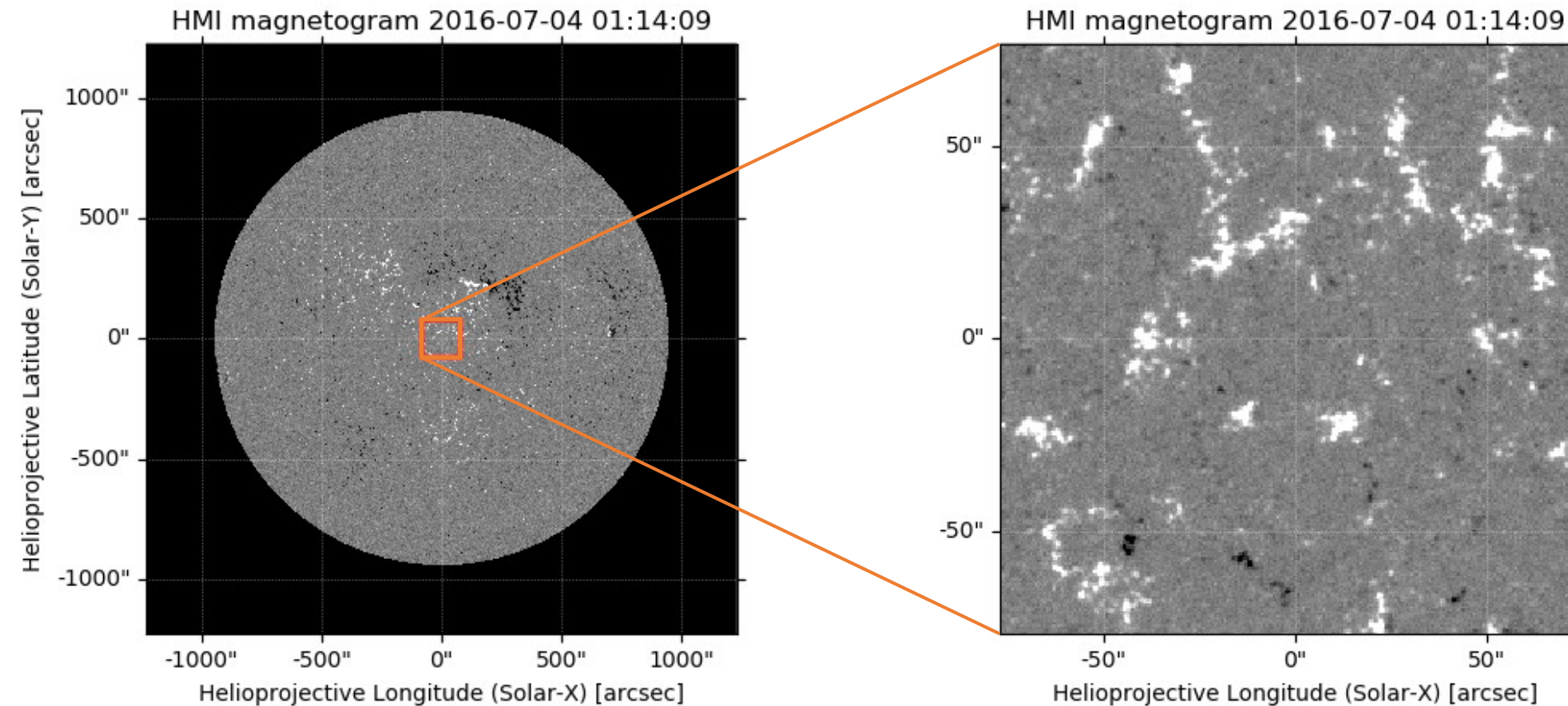
We design a deep learning model that translates from original magnetograms to corresponding denoised magnetograms.

-> We need pairs of the original magnetograms and the denoised magnetograms to train the model.

Denoising SDO/HMI Magnetogram

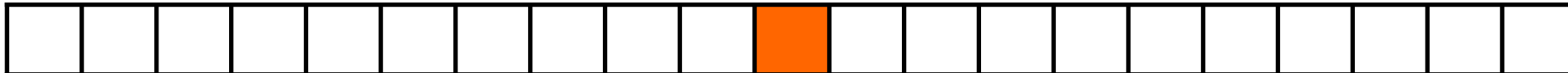
Crop patches from full disk HMI 45-second magnetogram

patch size: 256 x 256 (± 76.8 arcsec)



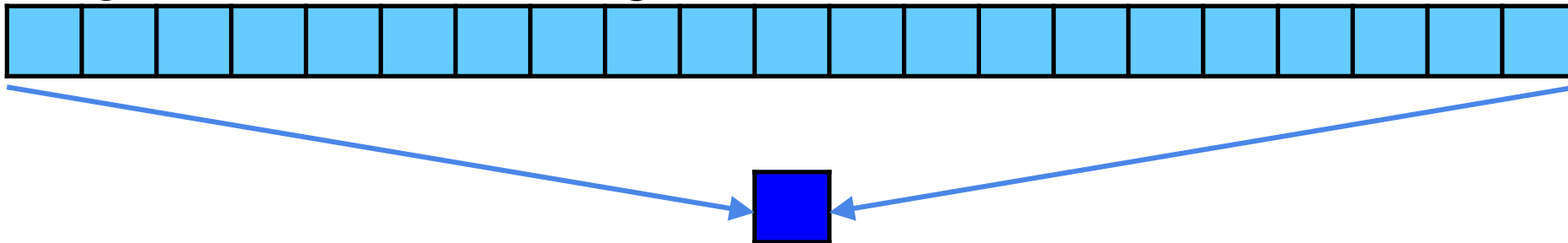
Denoising SDO/HMI Magnetogram

Input: Center frame Mag.



About 15 mins

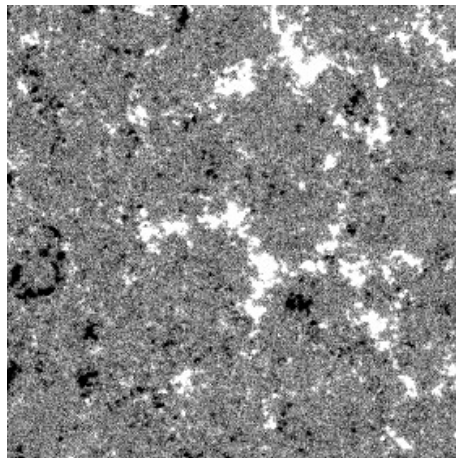
Target: 21-frame-stacked Mag.



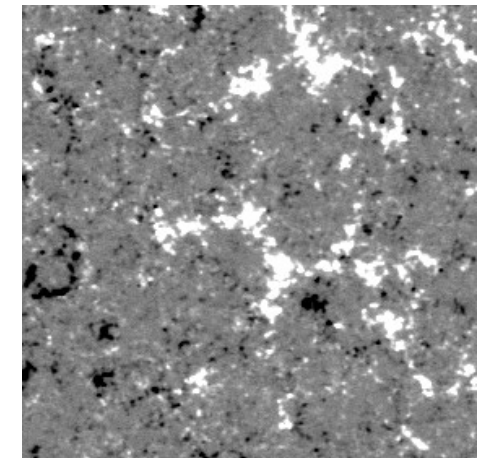
We integrate 21 magnetogram patches that include 10 frames before and 10 frames after the input magnetogram patch considering solar rotation. A stacked magnetogram has approximately 15 minutes of exposure time.

Denoising SDO/HMI Magnetogram

Original HMI
(Input)



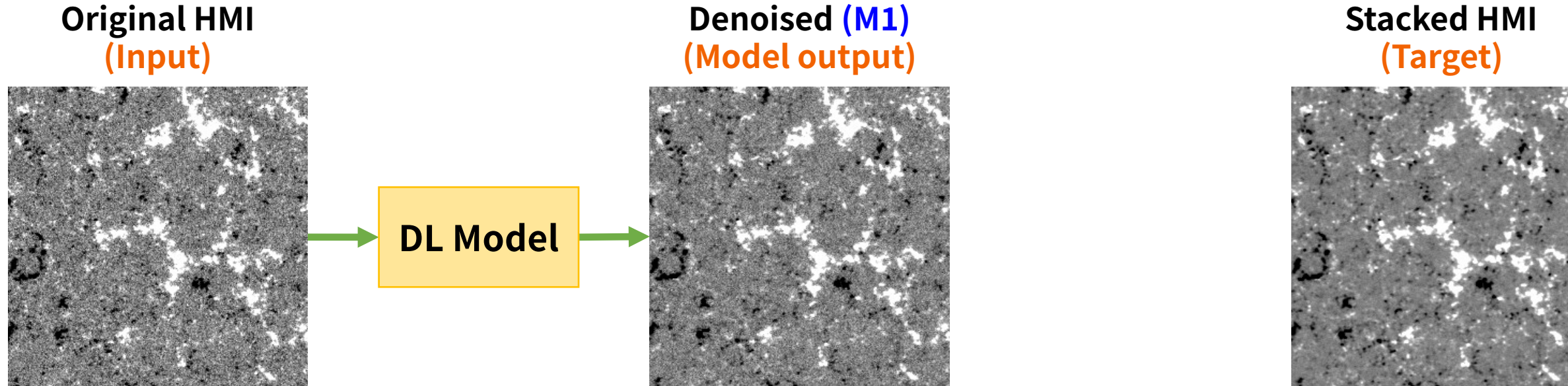
Stacked HMI
(Target)



DL Model

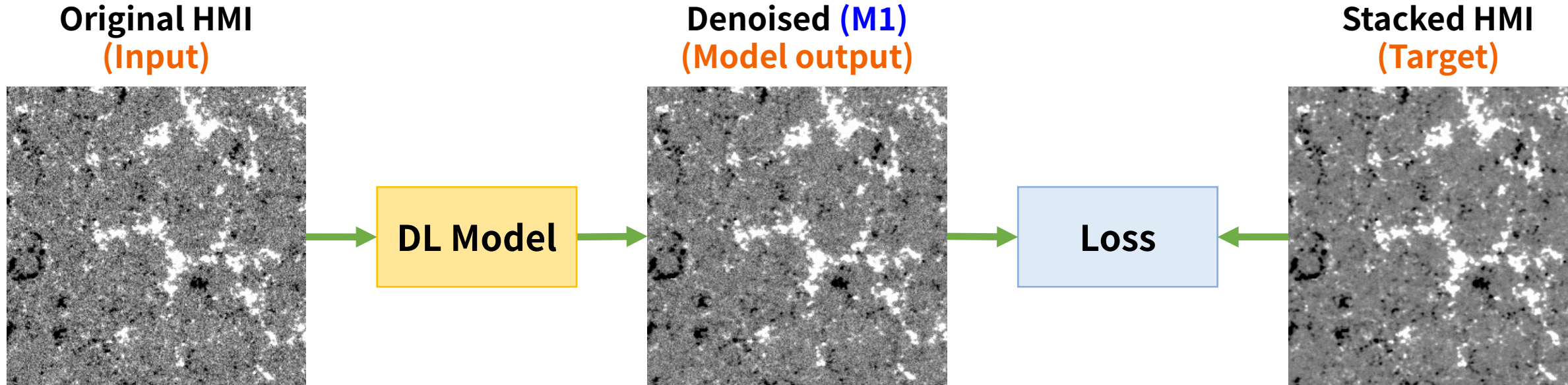
We prepare the pairs of the original magnetograms and the stacked magnetograms.

Denoising SDO/HMI Magnetogram



We prepare the pairs of the original magnetograms and the stacked magnetograms.
The model
1) generates the denoised magnetograms using the original magnetograms,

Denoising SDO/HMI Magnetogram

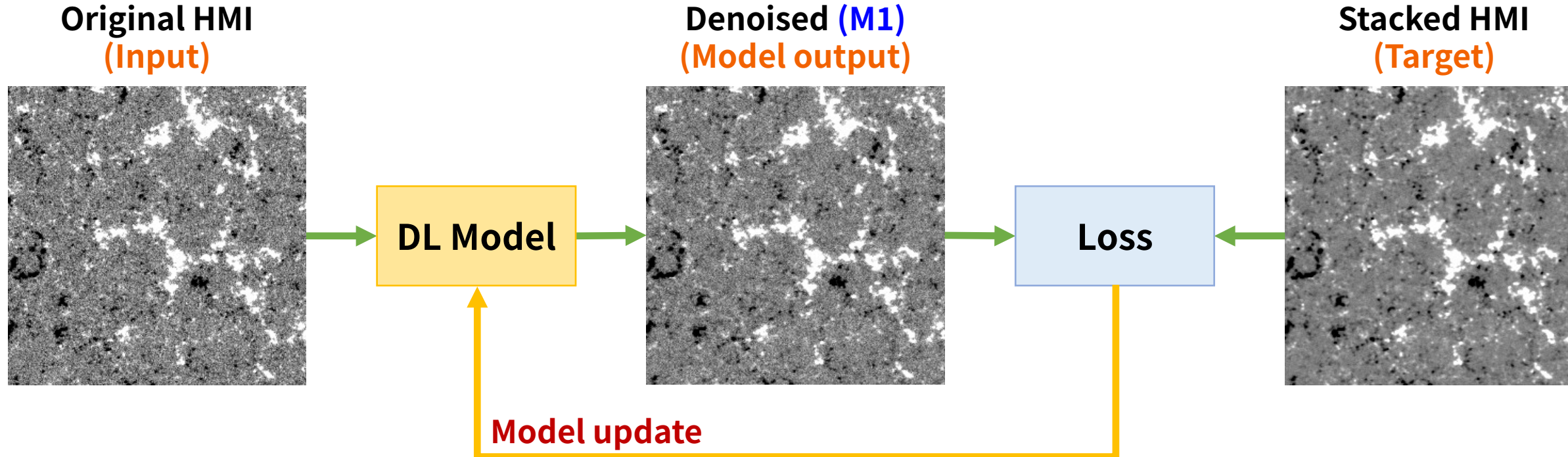


We prepare the pairs of the original magnetograms and the stacked magnetograms.

The model

- 1) generates the denoised magnetograms using the original magnetograms,
- 2) calculates the difference between the denoised and the stacked magnetograms,

Denoising SDO/HMI Magnetogram



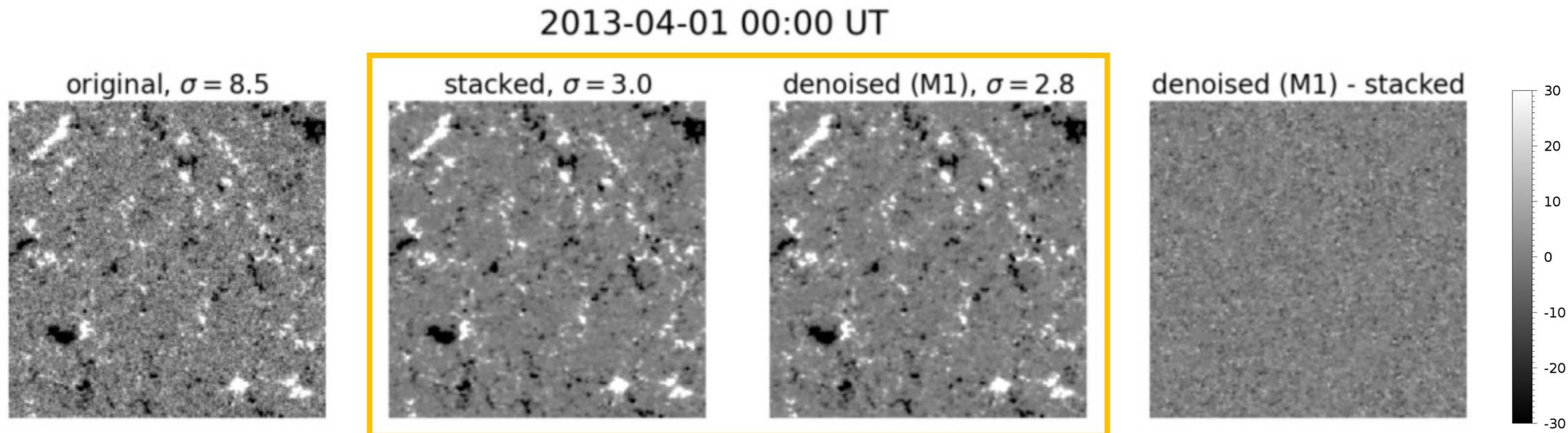
We prepare the pairs of the original magnetograms and the stacked magnetograms.

The model

- 1) generates the denoised magnetograms using the original magnetograms,
- 2) calculates the difference between the denoised and the stacked magnetograms,
- 3) back-propagates the difference, and updates itself to minimize the difference.

Denoising SDO/HMI Magnetogram

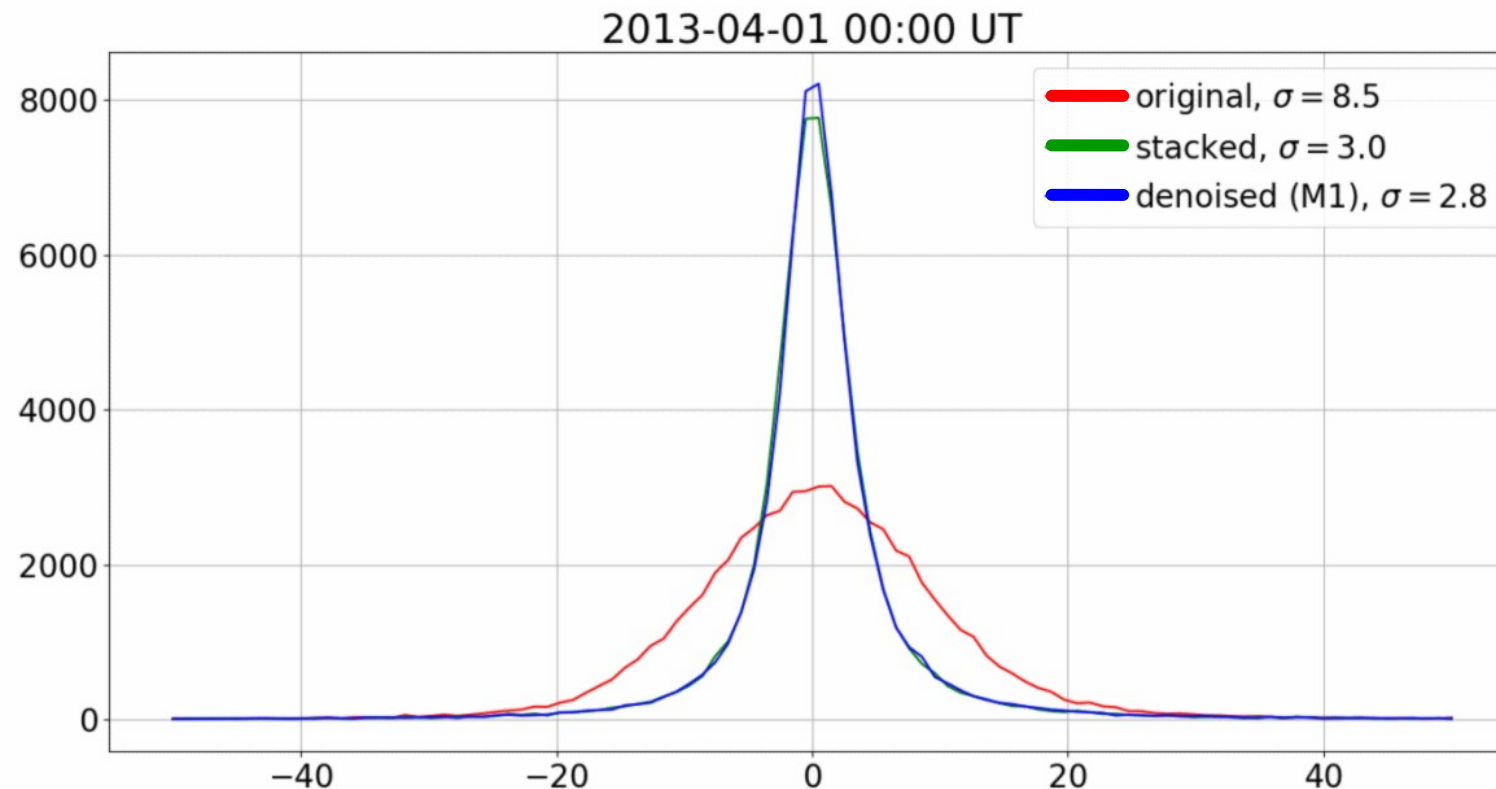
Comparisons between the original, stacked, and denoised magnetograms



The denoised magnetograms by our model are consistent with the stacked ones.

Denoising SDO/HMI Magnetogram

Histograms of magnetic flux densities from
the original, stacked, and denoised magnetograms



The histograms of the denoised magnetograms are similar to those of the stacked ones,
and their noise levels are almost same.

Denoising SDO/HMI Magnetogram

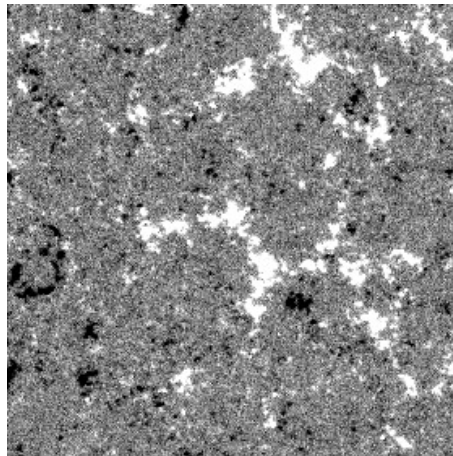
- Our model based on image translation method successfully reduce the noise level of SDO/HMI magnetograms.
- This method can be applied only when we have **pairs** of the original magnetograms (input) and the denoised magnetograms (target).
- The quality of the model outputs can be affected by the condition of the target data, such as the number of frames for the stacked magnetograms.

Denoising SDO/HMI Magnetogram

- Our model based on image translation method successfully reduce the noise level of SDO/HMI magnetograms.
- This method can be applied only when we have **pairs** of the original magnetograms (input) and the denoised magnetograms (target).
- The quality of the model outputs can be affected by the condition of the target data, such as the number of frames for the stacked magnetograms.
- We design an additional model (M2) based on AutoEncoder method that can train without target magnetograms.

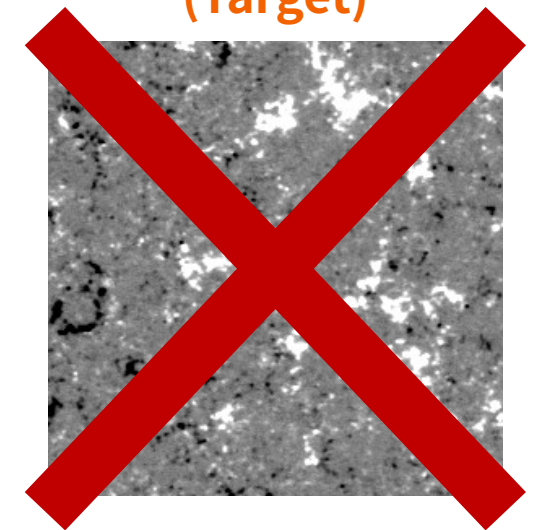
Denoising SDO/HMI Magnetogram

Original HMI
(Target)



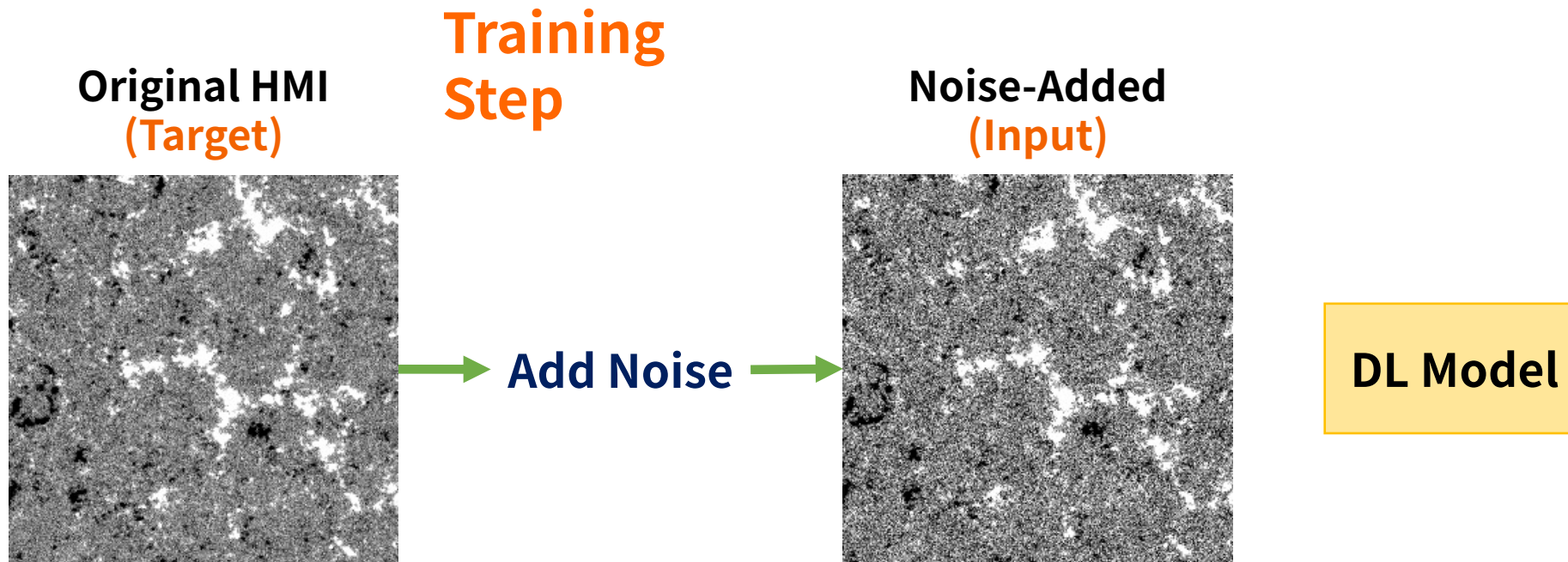
DL Model

Stacked HMI
(Target)



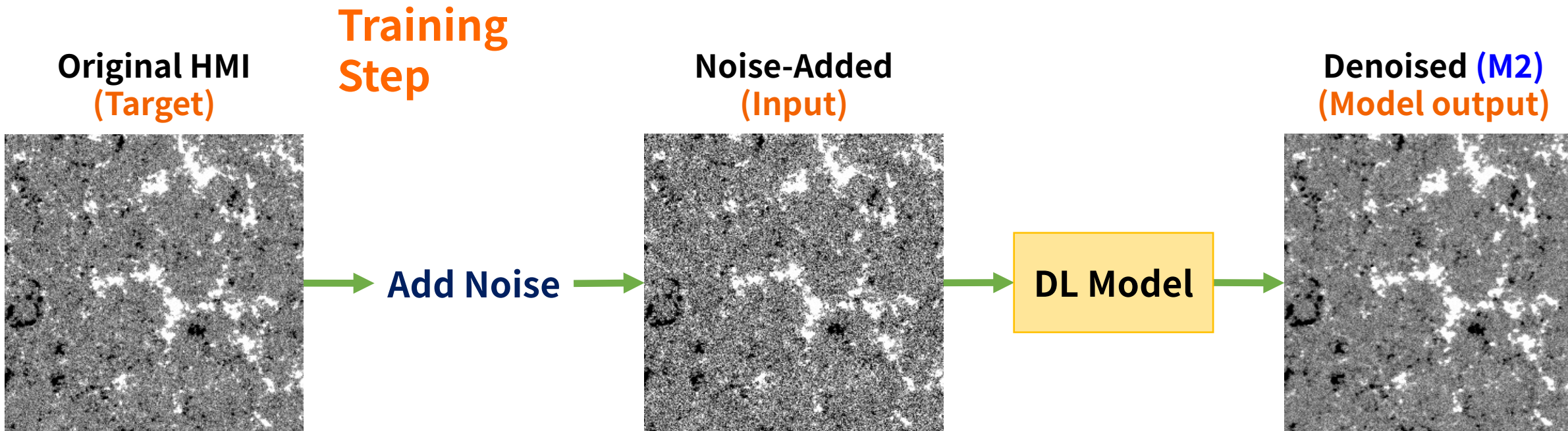
The dataset is the same as the previous study, but we will not use the stacked magnetograms.

Denoising SDO/HMI Magnetogram



We prepare the original magnetograms and add random Gaussian noise to the magnetograms. The noise distributions are similar to those of the original ones.

Denoising SDO/HMI Magnetogram

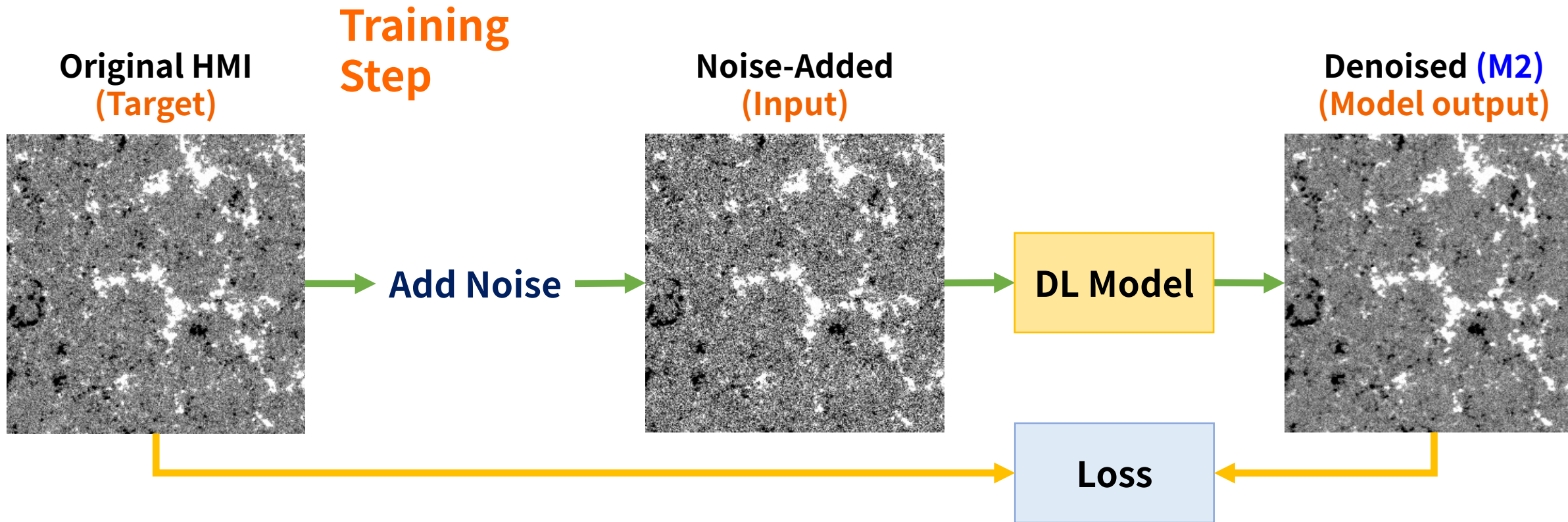


We prepare the original magnetograms and add random Gaussian noise to the magnetograms.

The model

- 1) generates the denoised magnetograms using the noise-added magnetograms,

Denoising SDO/HMI Magnetogram

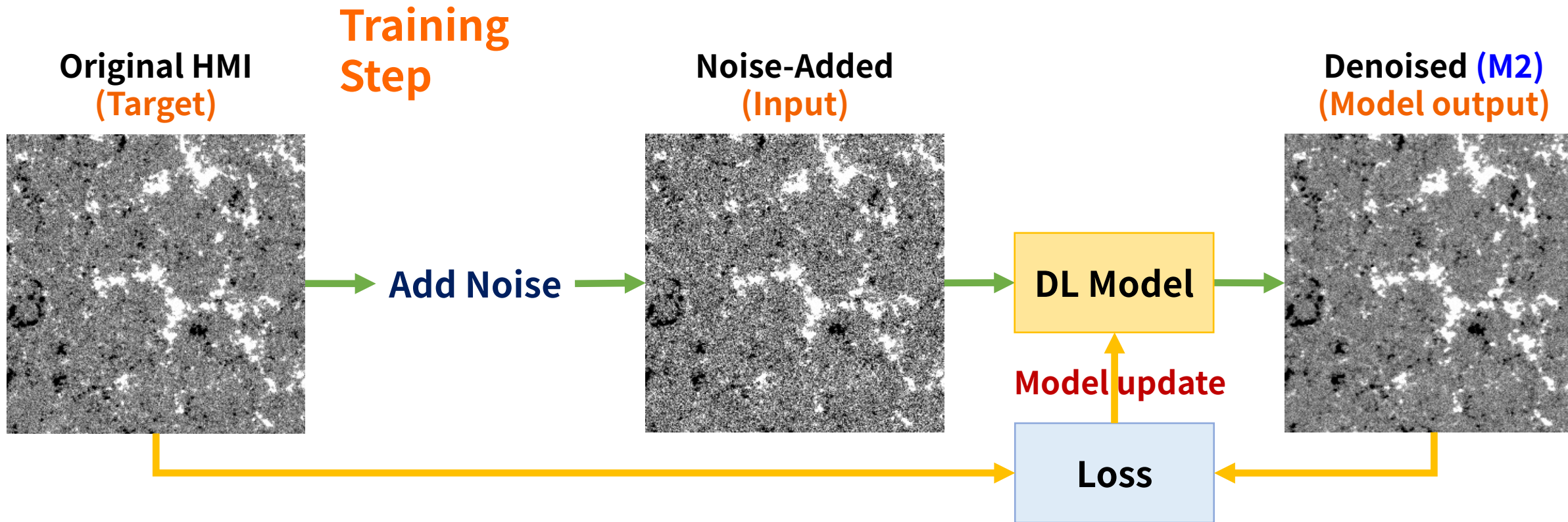


We prepare the original magnetograms and add random Gaussian noise to the magnetograms.

The model

- 1) generates the denoised magnetograms using the noise-added magnetograms,
- 2) calculates the difference between the denoised and the original magnetograms,

Denoising SDO/HMI Magnetogram



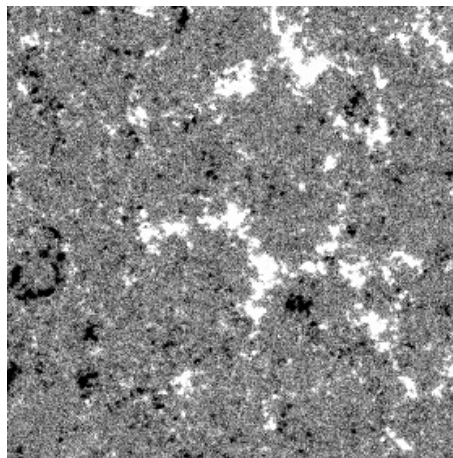
We prepare the original magnetograms and add random Gaussian noise to the magnetograms.

The model

- 1) generates the denoised magnetograms using the noise-added magnetograms,
- 2) calculates the difference between the denoised and the original magnetograms,
- 3) back-propagates the difference, and updates itself to minimize the difference.

Denoising SDO/HMI Magnetogram

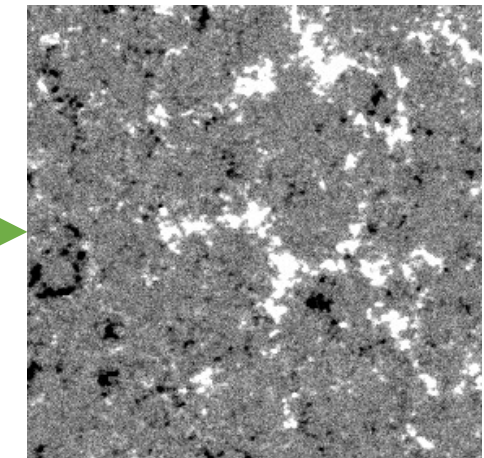
Original HMI
(Input)



Generation Step

DL Model

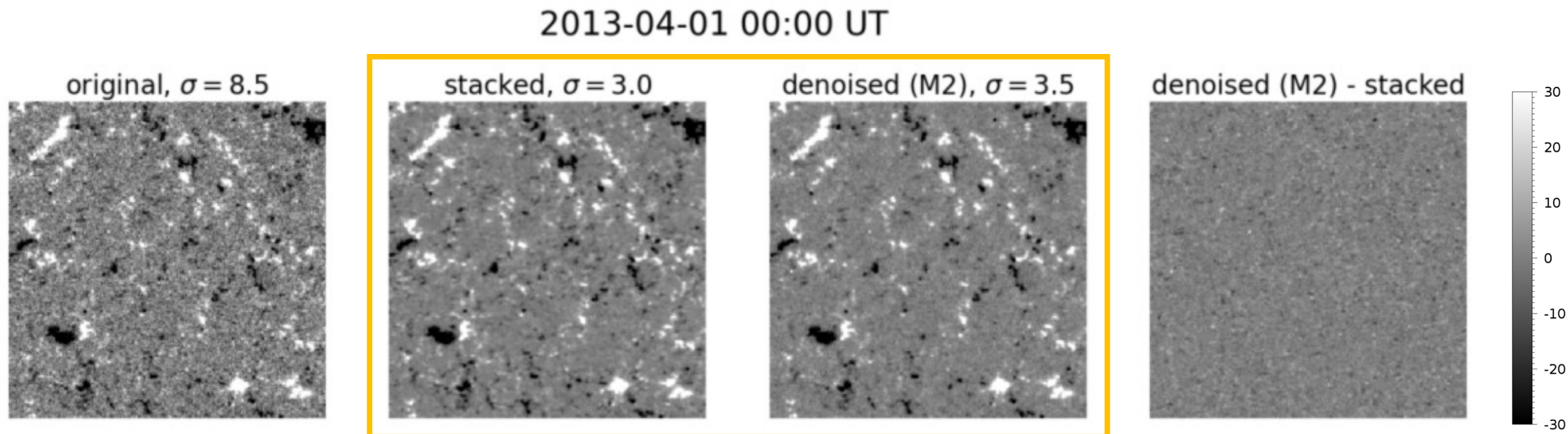
Denoised (M2)
(Model output)



The model generates the denoised magnetograms using the original magnetograms.

Denoising SDO/HMI Magnetogram

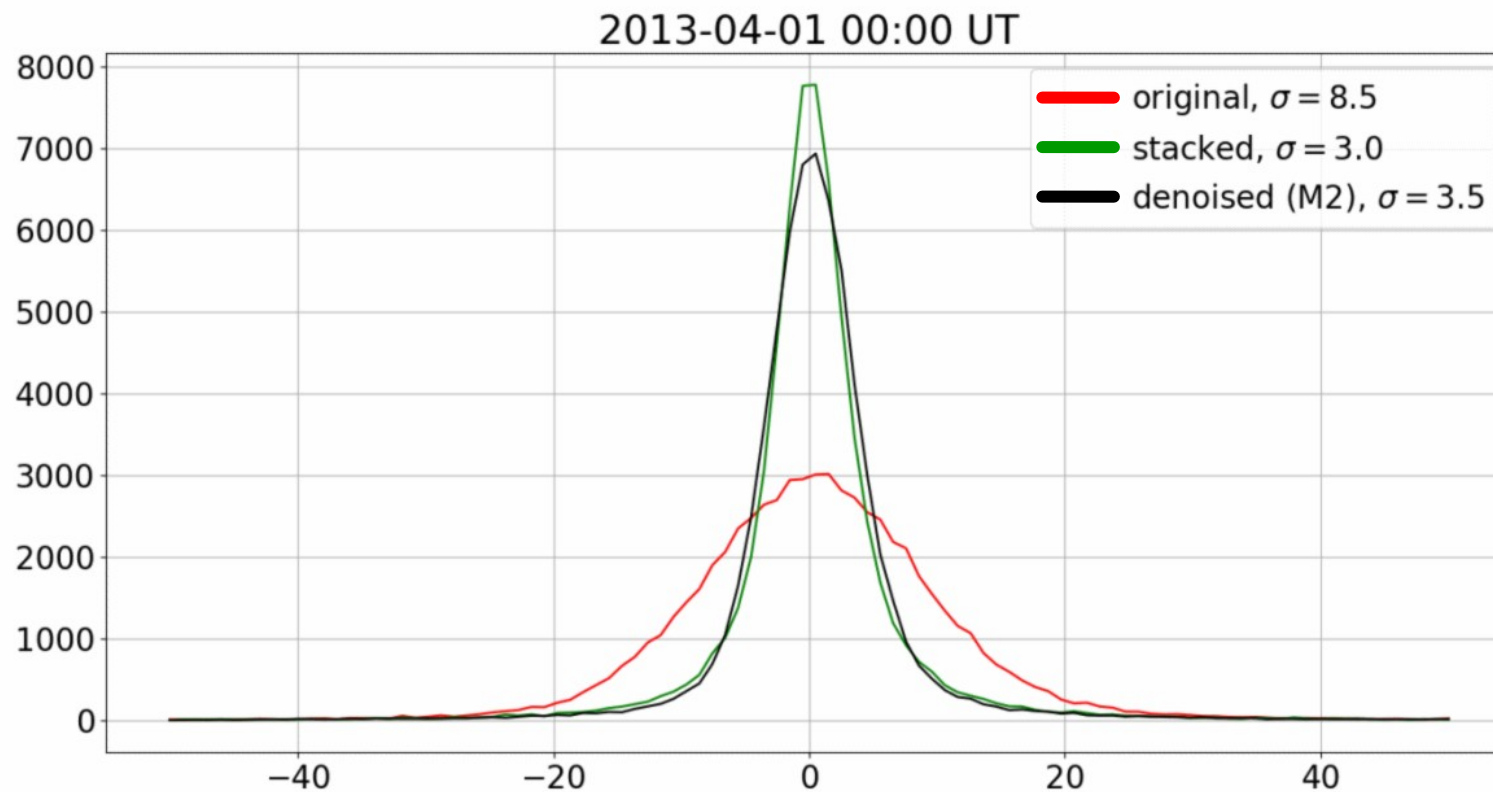
Comparisons between the original, stacked, and denoised magnetograms



The denoised magnetograms by our AutoEncoder model are consistent with the stacked ones

Denoising SDO/HMI Magnetogram

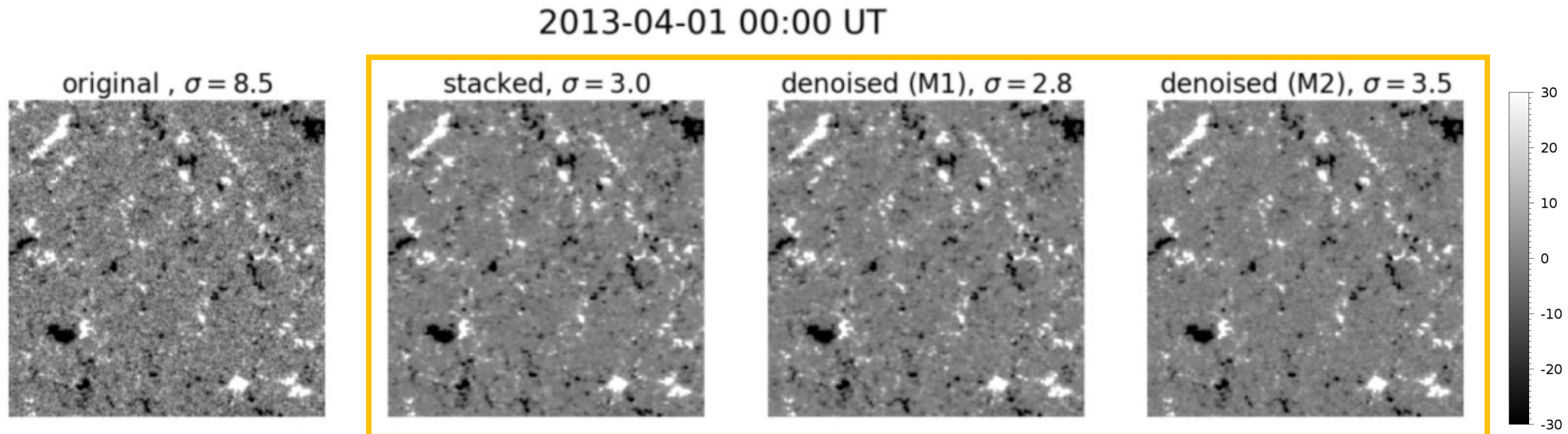
Histograms of magnetic flux densities from the original, stacked, and denoised magnetograms



The histograms of the denoised magnetograms are similar to those of the stacked ones

Denoising SDO/HMI Magnetogram

Comparisons between original, stacked, and denoised magnetograms by two models

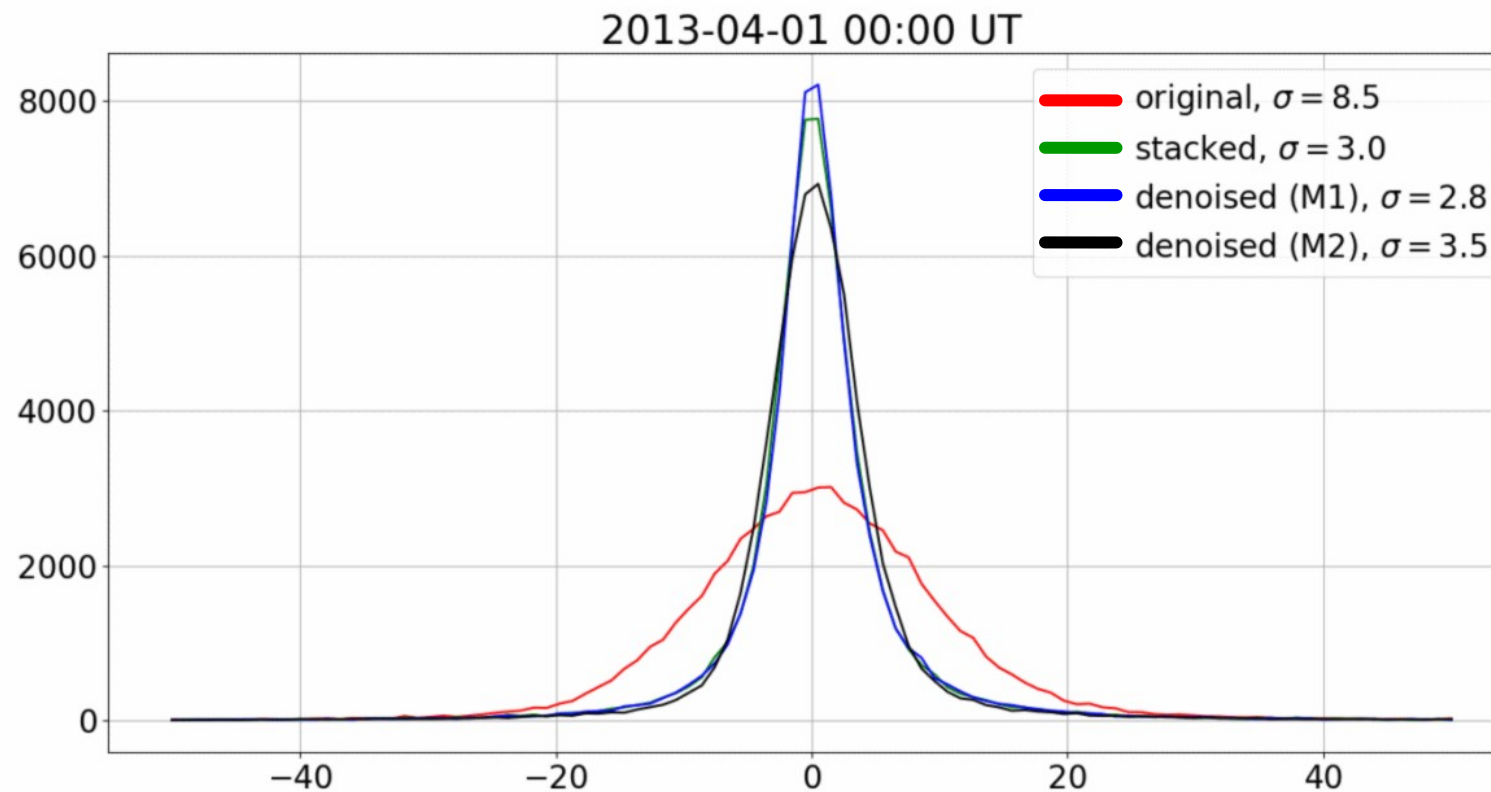


The denoised magnetograms by two models are consistent with each other.

M1: Image translation model, M2: AutoEncoder model

Denoising SDO/HMI Magnetogram

Histograms of magnetic flux densities from the original, stacked, and denoised magnetograms by two models



M1: Image translation model
M2: AutoEncoder model

The denoised magnetograms by the two models are similar to each other

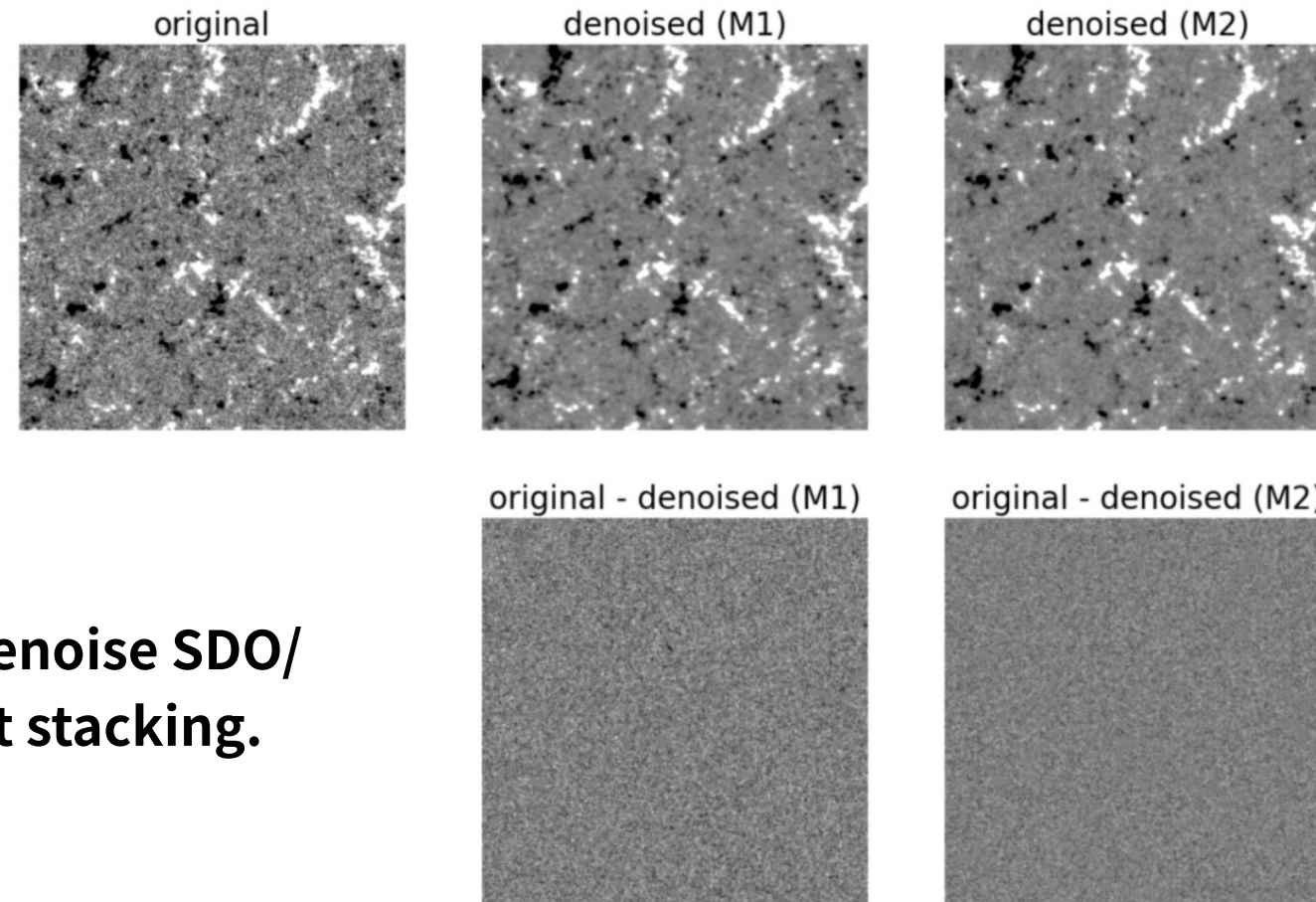
Denoising SDO/HMI Magnetogram

Application of our models to 21 frames of original SDO/HMI magnetograms

2013-04-15 22:00 UT

M1: Image translation model

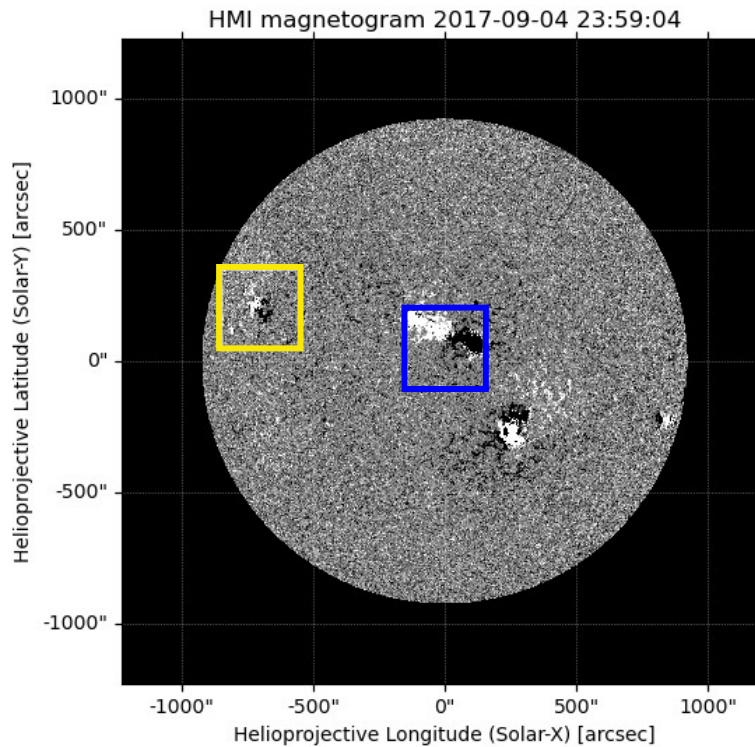
M2: AutoEncoder model



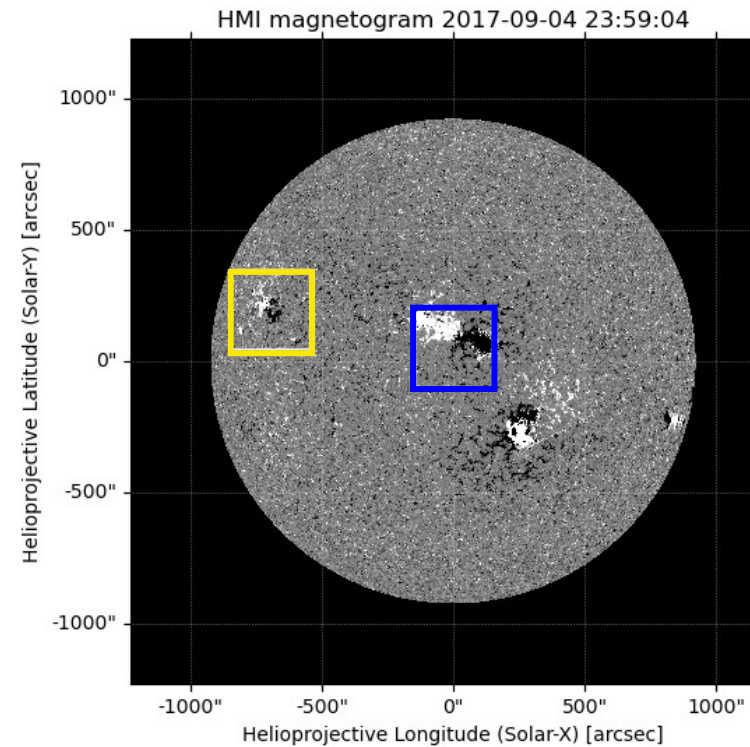
After the training, we can denoise SDO/
HMI magnetograms without stacking.

Denoising SDO/HMI Magnetogram

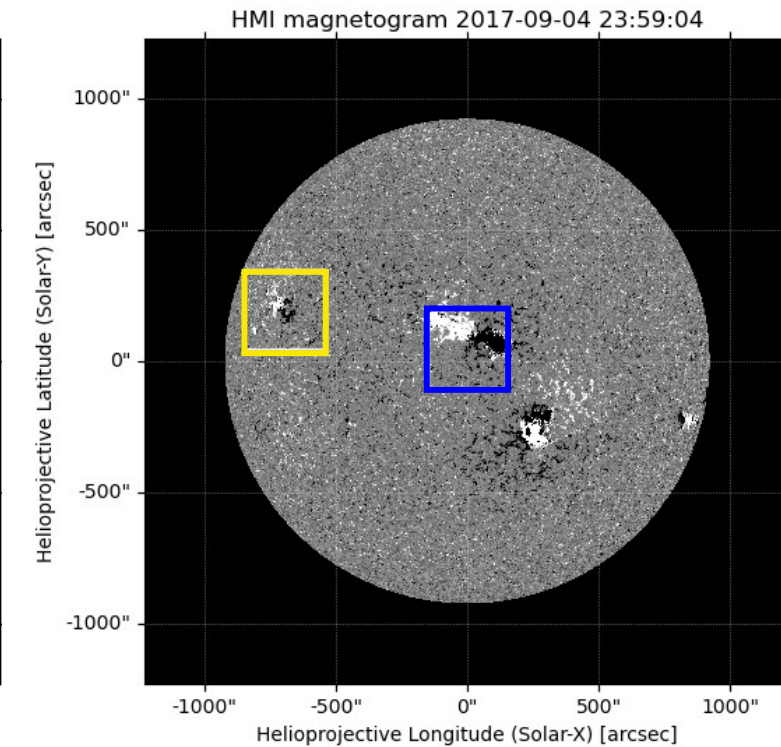
Application of our model to a full-disk SDO/HMI magnetogram



Original



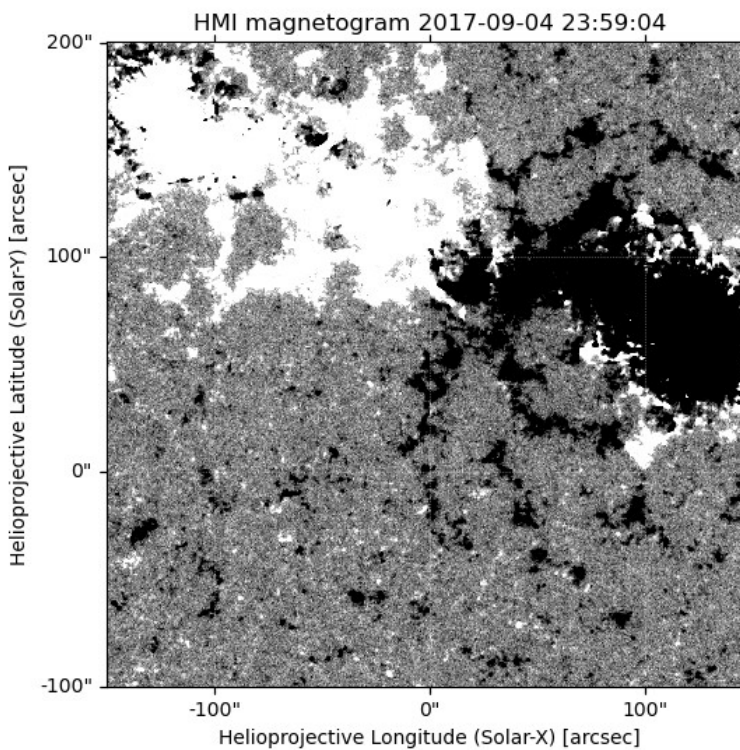
Denoised
(M1: Image Translation)



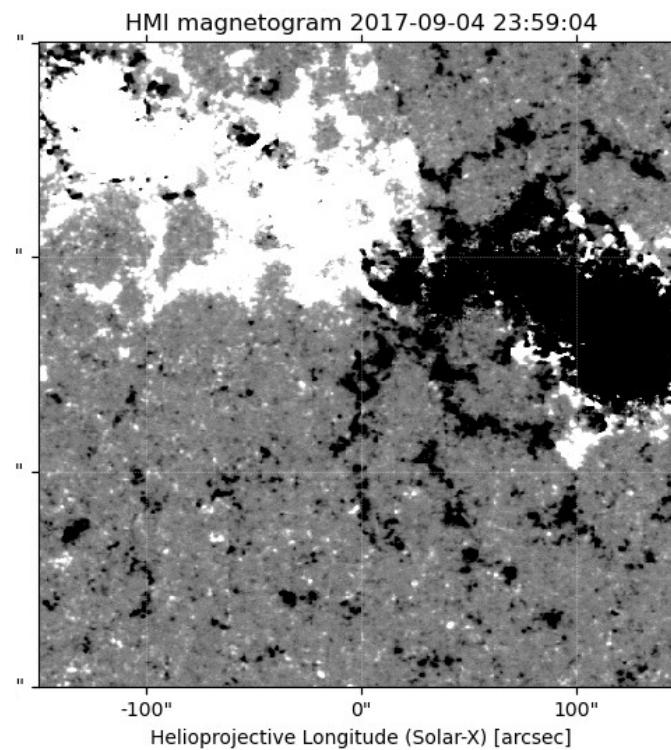
Denoised
(M2: AutoEncoder)

Denoising SDO/HMI Magnetogram

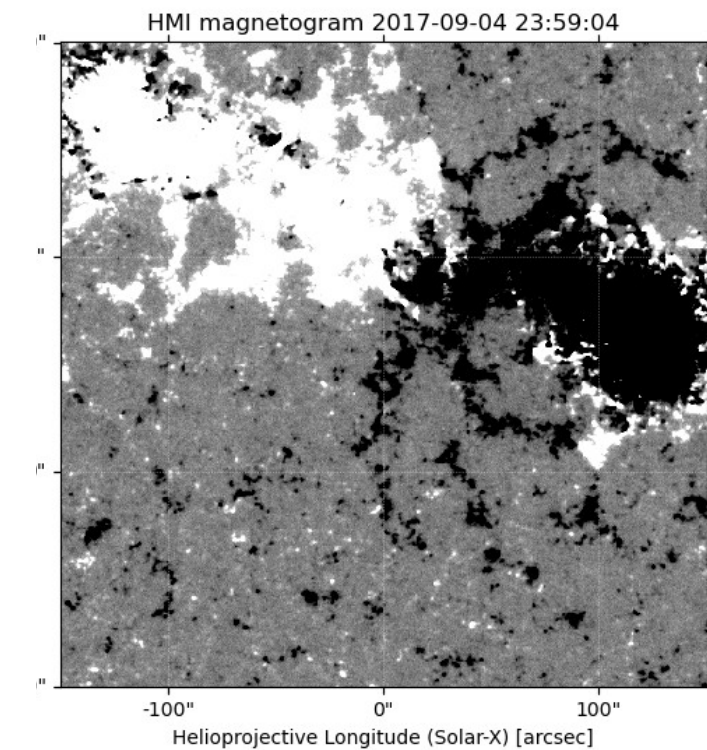
Application of our model to a full-disk SDO/HMI magnetogram: center of disk



Original, noise level: 9.1 G



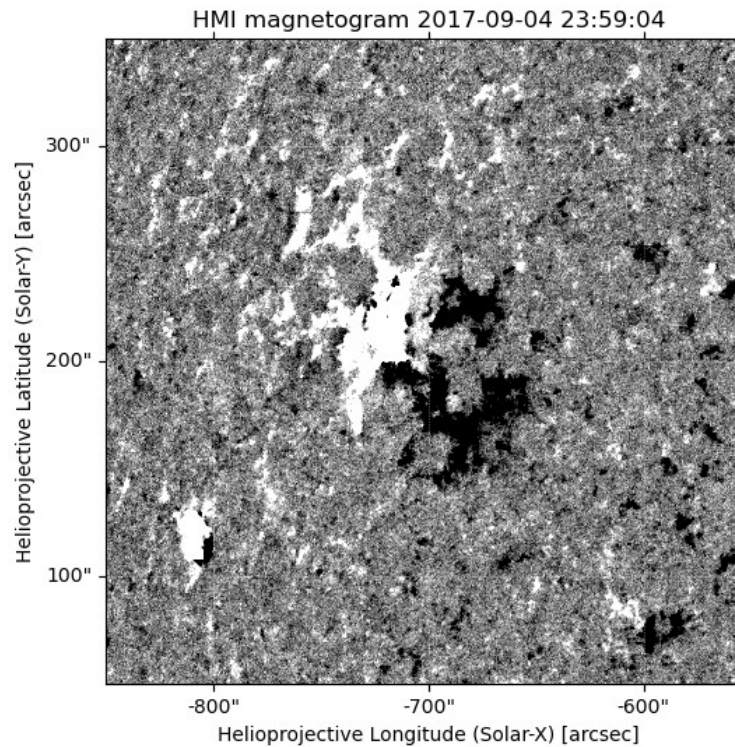
Denoised, noise level: 3.4 G
(M1: Image Translation)



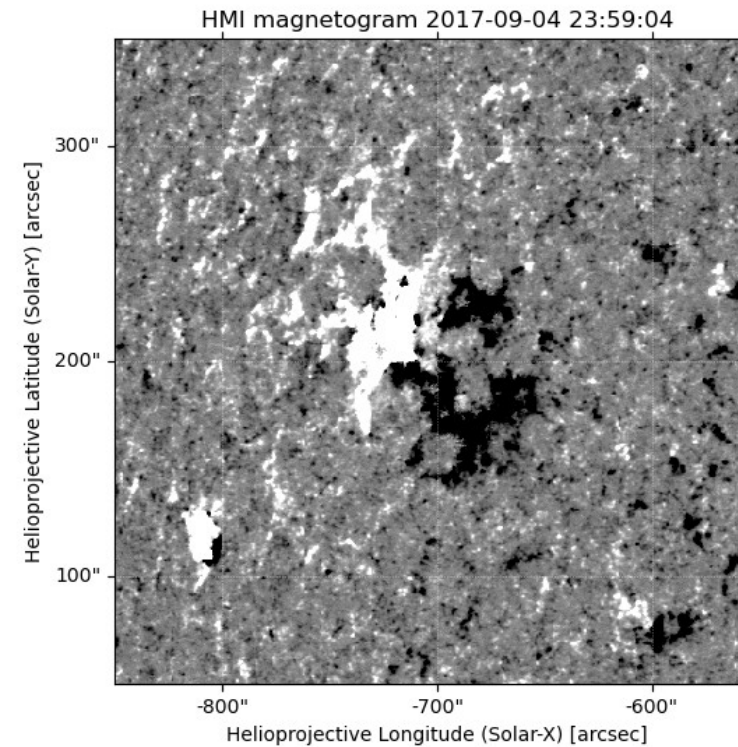
Denoised, noise level: 3.9 G
(M2: AutoEncoder)

Denoising SDO/HMI Magnetogram

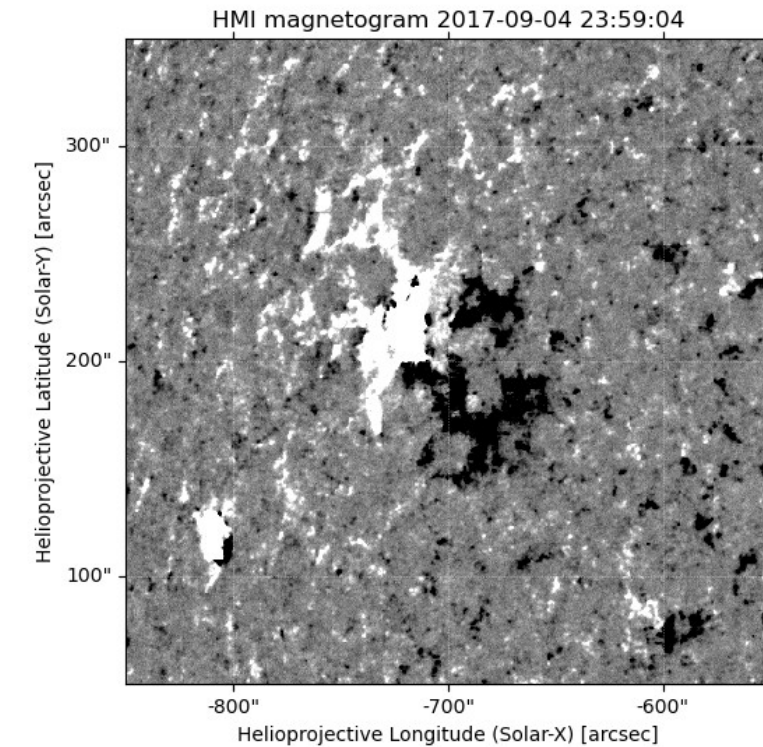
Application of our model to a full-disk SDO/HMI magnetogram: near the limb



Original, noise level: 10.7 G



Denoised, noise level: 4.5 G
(M1: Image Translation)



Denoised, noise level: 4.9 G
(M2: AutoEncoder)

Denoising SDO/HMI Magnetogram

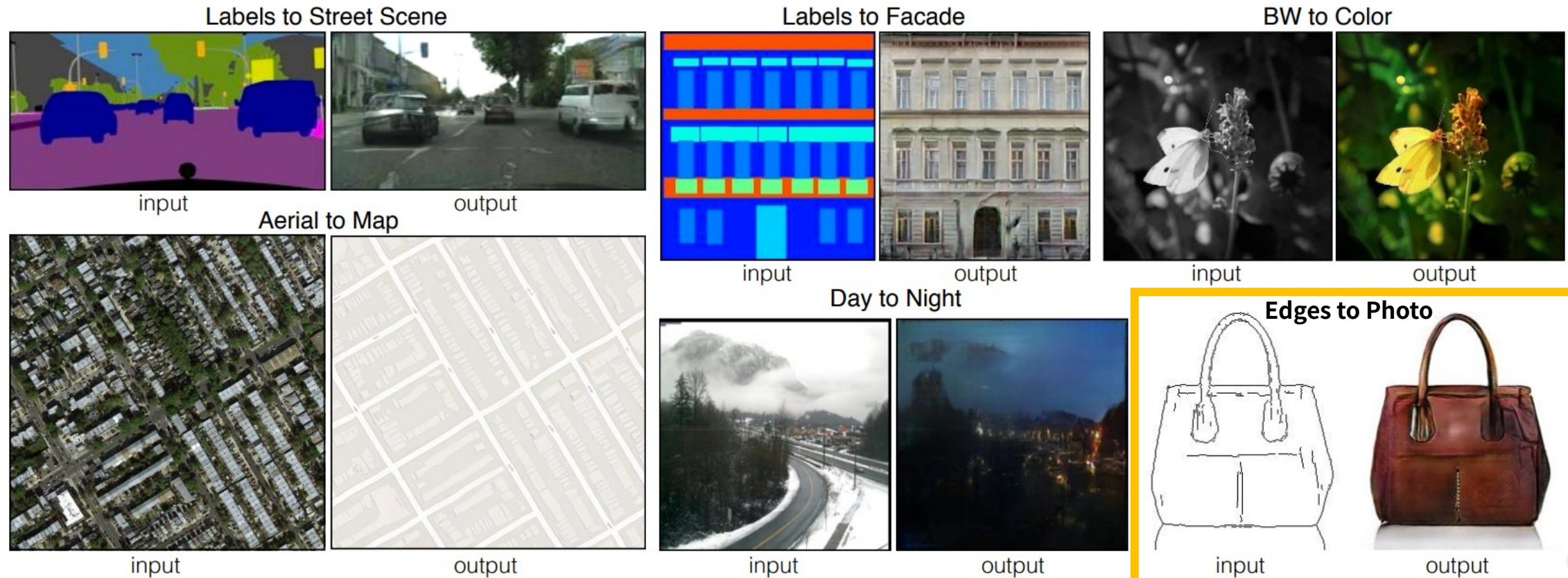
- The **image-translation method** can be applied to denoising solar and space weather data if **we can build many target noise-reduced data**.
- If it is **difficult to build the denoised target data**, the **AutoEncoder method** can be applied to denoising solar and space weather data as an alternative.

3

Generation of Modern Satellite Images from Galileo sunspot drawings in 1612

Lee et al., 2021

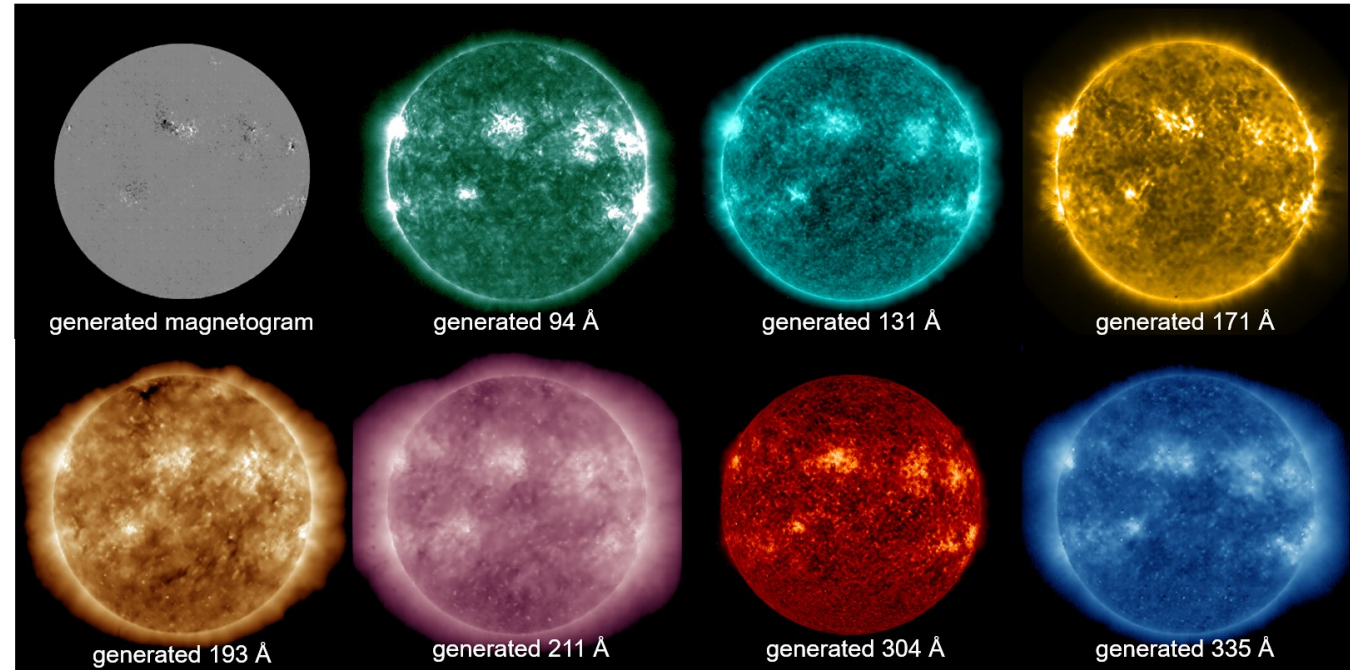
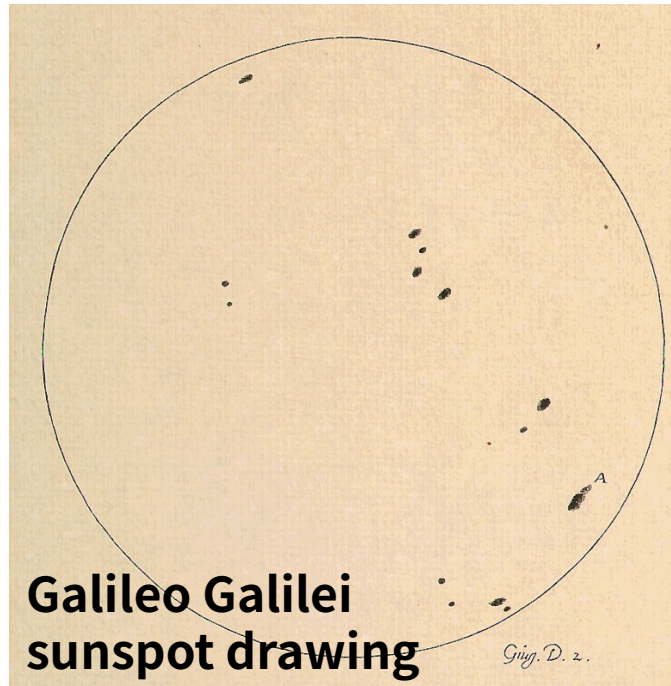
Generation of Satellite Image from Galileo Sunspot



Isola et al. 2017

We have similar data to this example, that is sunspot drawings.

Generation of Satellite Image from Galileo Sunspot



http://galileo.rice.edu/sci/observations/sunspot_drawings.html

poster session

Title: Generation of Modern Satellite Data from Galileo Sunspot Drawings by Deep Learning

Author: Harim Lee

THANK YOU



KYUNG HEE
UNIVERSITY